

POLITECNICO DI TORINO

Master of Science in Energy and Nuclear Engineering

Master Degree Thesis

Techno-economic analysis and improvement of the carbonator side heat exchanger network for the Calcium-Looping indirect integration with a supercritical Organic Rankine Cycle in a Concentrated Solar Power plant



Supervisors:

prof. Vittorio Verda
prof. Elisa Guelpa
dott. Tesio Umberto

Candidate:

Fabrizio Viti

December 2019 (Academic Year 2018/2019)

Table of contents

1 Introduction	1
2 General aspects of the SOCRATCES project.....	3
2.1 Introduction about thermal energy storage (TES).....	3
2.1.1 Sensible heat storage.....	3
2.1.2 Latent heat storage.....	4
2.1.3 Chemical heat storage	4
2.1.4 Comparison between different types of storage.....	5
2.2 The Calcium-Looping (CaL) process	6
2.3 Description of the technology involved for the plant components	10
2.3.1 Solids conveying technology.....	11
2.3.2 Carbonator	12
2.3.3 Calciner.....	14
2.3.4 Storages.....	15
2.3.5 Gas turbine technology.....	16
2.3.6 Heat exchangers.....	17
2.4 SOCRATCES goals to achieve.....	19
3 CSP-CaL integration with power cycles.....	20
3.1 Direct integration	20
3.2 Indirect integration	23
3.3 Organic Rankine Cycle (ORC)	26
4 Heat exchanger network design	31
4.1 Optimization of the ORC integration	31
4.2 A first design of the heat exchange network.....	33
4.3 Linearization of heat capacities and design simplification	39

5 Economic improvement of the heat network.....	44
5.1 Simplification of the heat exchangers network.....	44
5.2 Economic analysis of the obtained networks.....	52
5.2.1 Estimation of the BEC.....	54
5.2.2 Estimation of the EPCC.....	59
5.2.3 Estimation of TPC.....	60
5.2.4 Estimation of TOC.....	60
5.2.5 Estimation of TASC.....	61
5.2.6 Estimation of WACC.....	63
5.2.7 Calculation of the fuel flowrate and combustion chamber volume.....	65
5.2.8 Evaluation of the LCOE.....	68
5.3 Results and final comments.....	69
Conclusions.....	77
References.....	78
Ringraziamenti.....	84

1 Introduction

Nowadays climate changes due to human activities are the main topics concerning the biggest political decisions worldwide; in all these discussions, one of the most widespread solution is the production of energy from decarbonized sources in parallel with an improvement of the already existing power plants based on fossil fuels, aiming at a reduction of greenhouse gases (GHG) emissions.

For these reasons, the renewable energy sources (RES) are assuming more and more importance in the satisfaction of the global energy demand: every year the percentage of the total amount of energy produced by them is increasing and many projects and studies are carried out to improve plants' efficiencies and to obtain optimal configurations and parameters for the production.

However, there are also some drawbacks related to RES; one of the most important in their development and spreading is the discontinuity and the discrepancy between energy production and demand (more influent in case of solar energy production, since there is overproduction during the day and underproduction during the night). To solve these issues, it is gaining a fundamental role to match energy production with appropriate storage systems; this solution has been studied for several applications, but in particular for Concentrated Solar Power (CSP) plants, where heat from solar source is utilized to produce electric power in a thermodynamic cycle.

One of the most interesting project developed in this sector is SOCRATCES (SOlar Calcium-looping integRAtion for Thermo-Chemical Energy Storage), in which a CSP plant is coupled with a Thermo-Chemical Energy Storage (TCES) based on Calcium Looping (CaL): it is a chemical looping in which heat is required to obtain CO₂ and calcium oxide (CaO) from calcium carbonate (CaCO₃) by calcination and in which this heat is subsequently released by the reverse reaction of carbonation. The main difference between this project and the other ones conducted in the carbon capture and sequestration (CCS) field, is that the operating conditions under investigations are chosen in order to solve some traditional CaL issues and to maximize power production and efficiency.

The objective of this thesis is to analyse the optimal configuration for heat recovery network devoted to the discharge process, to further simplify the obtained network and to carry out an economic analysis of the obtained designs with the aim of find the optimal compromise between heat exchanger network complexity due to 100% renewable operating conditions and the costs associated to the use of external

heating sources. All the simulations and considerations that are contained in this study has been developed using the software Aspen Plus V8.8 and, particularly, the tool Energy Analyzer in it.

2 General aspects of the SOCRATCES project

2.1 Introduction about thermal energy storage (TES)

As already introduced, energy storage is one of the most important solution in order to make the production from RES feasible and competitive on the market. In CSP applications, heat (and mostly its full exploitation) plays a fundamental role, so thermal energy storages (TES) could be integrated in order to exploit solar radiation as much as possible and to guarantee a continuous power production, avoiding peaks and shortage.

Thermal energy storages can be mainly of three types ([1], [2] and [3]) :

- 1) Sensible heat storage
- 2) Latent heat storage
- 3) Chemical heat storage

2.1.1 Sensible heat storage

In sensible heat storages, sensible heat is used to increase the temperature of a fluid or solid medium, increasing therefore its energy content. The sensible heat (Q) that is stored into the medium can be expressed as:

$$Q = m \cdot \bar{c}_p \cdot \Delta T = \rho \cdot V \cdot \bar{c}_p \cdot \Delta T \quad (1)$$

being m, ρ and V respectively the mass, the density and the volume of the medium, \bar{c}_p the average specific heat between extreme temperatures and ΔT the temperature variation caused by heat storage.

In this type of storage, heat losses are relevant, so a suitable insulation must guarantee high thermal efficiencies and performances. Most used liquid media are molten salts and mineral oils, for which stratification, required in order to reduce losses, is ensured by avoiding mixing of layers with different temperatures. For solid media, CSP applications exploit mainly concrete and castable ceramics, because of their easy processing and low costs; nevertheless, even if some thermal and mechanical properties are good at high temperatures, other thermal properties could get worse because of the increase in temperature, so this type of storage presents some important drawbacks in our applications. Anyway, this type of storage for CSP plants has been fully studied in recent years ([4]- [5]).

2.1.2 Latent heat storage

For this type of storage, during charge the solar radiation is used as a heat source for phase change of the medium (that, for this reason, it's called Phase Changing Material (PCM)), so heat transfer takes place approximately at constant temperature; during discharge, heat stored is released under the form of latent heat, so that medium returns to the initial state. The reference equation for these phenomena is:

$$Q = m \cdot \lambda = \rho \cdot V \cdot \lambda \quad (2)$$

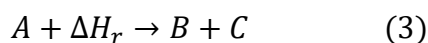
where λ is the latent heat linked to the phase change [J/kg].

These systems work with smaller temperature differences between charging and discharging phase and have a higher energy density with respect to sensible heat storages; however, in order to obtain a high-quality heat, phase change temperature must be sufficiently high, increasing thus heat losses. Scientific literature is full of studies about this type of storage ([6]- [7])

2.1.3 Chemical heat storage

For this type of storage, also defined as thermochemical energy storage (TCES), reversible reactions are involved. During charging phase, heat from solar source is used to run an endothermic reaction from which products are stored; when energy is needed, they can be recombined, obtaining the original substances and releasing thus the energy stored in form of heat.

Assuming a general reaction involved in these systems:



the resulting equation used to assess the energy involved is the following:

$$Q = n_A \cdot \Delta H_r \quad (4)$$

where n_A is the number of moles of the reactant A and ΔH_r is the molar heat of reaction referred to A [J/mol].

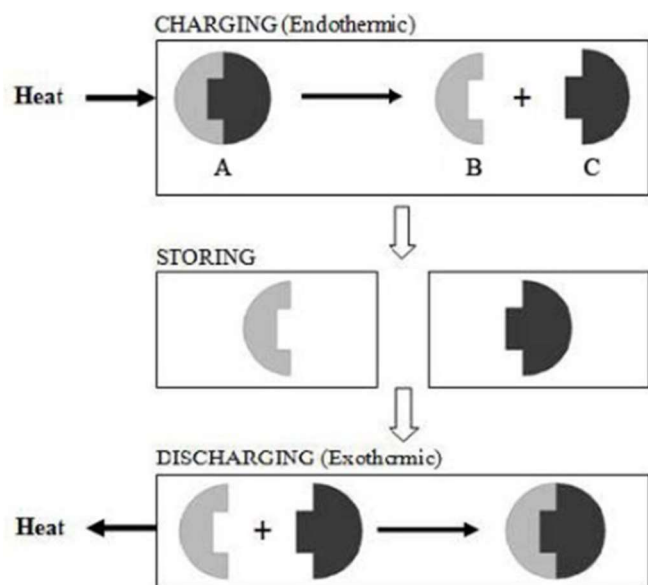


Figure 1-Conceptual scheme of the functioning of a chemical heat storage [44]

2.1.4 Comparison between different types of storage

To compare the three different TES systems, 6 parameters are considered, as reported in the table below:

	Sensible heat storage system	Latent heat storage system	Thermochemical storage system
Energy density			
Volumetric density	Small $\sim 50 \text{ kWh m}^{-3}$ of material	Medium $\sim 100 \text{ kWh m}^{-3}$ of material	High $\sim 500 \text{ kWh m}^{-3}$ of reactant
Gravimetric density	Small $\sim 0.02\text{--}0.03 \text{ kWh kg}^{-1}$ of material	Medium $\sim 0.05\text{--}0.1 \text{ kWh kg}^{-1}$ of material	High $\sim 0.5\text{--}1 \text{ kWh kg}^{-1}$ of reactant
Storage temperature	Charging step temperature	Charging step temperature	Ambient temperature
Storage period	Limited (thermal losses)	Limited (thermal losses)	Theoretically unlimited
Transport	Small distance	Small distance	Distance theoretically unlimited [12]
Maturity	Industrial scale	Pilot scale	Laboratory scale
Technology	Simple	Medium	Complex

Table 1-Characteristics and comparison of the thermal energy storage systems [8]

As it can be observed, thermochemical energy storages are the best choice for different reasons:

- products of endothermic reaction can be stored at ambient temperature, so there's no need of insulated vessels;
- lower temperatures mean also lower heat losses and thus a longer storage period;
- these systems are characterised by higher energy densities compared to sensible and latent heat storages, so in terms of compactness and amount of medium mass they represent a better choice.

The main drawback linked to this technology is the maturity, since it is still at a laboratory scale, but the potential is very high, and it can represent the future of thermal storages.

Between all the possible choices for the medium, calcium carbonate constitutes the best option in terms of operating temperature and energy density, as it can be seen from table below. In addition, the possibility to exploit limestone (an abundant, cheap and non-toxic material) as CaO precursor increases the interest for this application.

Thermal energy storage methods	Operating temp (°C)	Energy density (MJ/m ³)	Ref.
<i>Sensible heat</i>			
Silicone oil	300–400 °C	189	Gil et al. (2010)
Nitrite salts	250–450 °C	548	
Nitrate salts	265–565 °C	898	
Carbonate salts	450–850 °C	1512	
Liquid sodium	270–530 °C	287	
<i>Latent heat – high temp molten salts</i>			
	Phase change temp		
Sodium nitrite NaNO ₂	270 °C	373	Tamme et al. (2008)
Sodium nitrate NaNO ₃	307 °C	389	Gil et al. (2010)
Potassium nitrate KNO ₃	333 °C	561	Pincemin et al. (2008)
Sodium carbonate Na ₂ CO ₃	854 °C	701	Hoshi et al. (2005)
<i>Thermochemical</i>			
Iron carbonate FeCO ₃ – FeO + CO ₂	180 °C	2600	N'Tsoukpoe et al. (2009)
Calcium hydroxide, Ca(OH) ₂ –CaO + H ₂ O	500 °C	3000	Gil et al. (2010)
Calcium carbonate, CaCO ₃ –CaO + CO ₂	800–900 °C	4400	Gil et al. (2010)

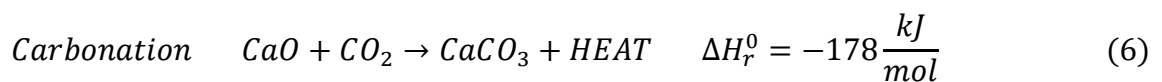
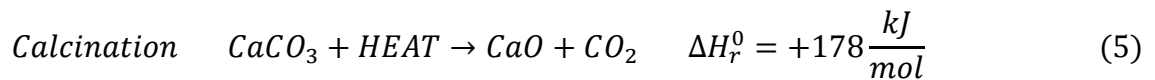
Figure 2-Comparison of high temperature heat storage materials [18]

2.2 The Calcium-Looping (CaL) process

As already observed, calcium carbonate and Calcium-Looping (CaL) process is very advantageous for TES applications; in particular, for CSP systems it is a promising choice for different reasons ([8] and [3]):

- there is no need of a catalyst for reactions;
- it has a very high energy density compared to other media (692 kWh/m³ of CaCO₃);
- materials involved are very cheap and relatively easy to obtain and to manage (limestone is one of the most common materials on Earth);
- most technologies involved with these materials are fully developed and well-proved on large scale;
- it is suitable for medium-high temperature storage.

Calcium-Looping is composed of two steps: in the first one (called calcination) heat from solar source is provided to a reactor (called calciner), where from calcium carbonate are obtained (and stored) calcium oxide and carbon dioxide; in the carbonator the reverse reaction (called carbonation) takes place, thus calcium carbonate and heat are obtained from the stored reactants.



This process has been widely studied in Carbon Capture and Sequestration (CCS) applications; however, operating conditions here imposed are not the most suitable ones for CaL process and present some important drawbacks. To understand it, we must take into consideration both reactions: from Le Châtelier's principle, we know that carbonation is enhanced by high reactants' pressure (in our case, high CO₂ partial pressure) and low temperature, whereas it is the opposite for the calcination. Moreover, from thermochemical data it is possible to obtain a formula which correlates temperature and pressure in equilibrium conditions [9]:

$$P_{eq}(\text{bar}) = P \cdot y_{eq} = \left[4,137 \cdot 10^7 \cdot \exp\left(-\frac{20,474}{T}\right) \right] \quad (7)$$

All these concepts can be well summarized by the following graph [10]:

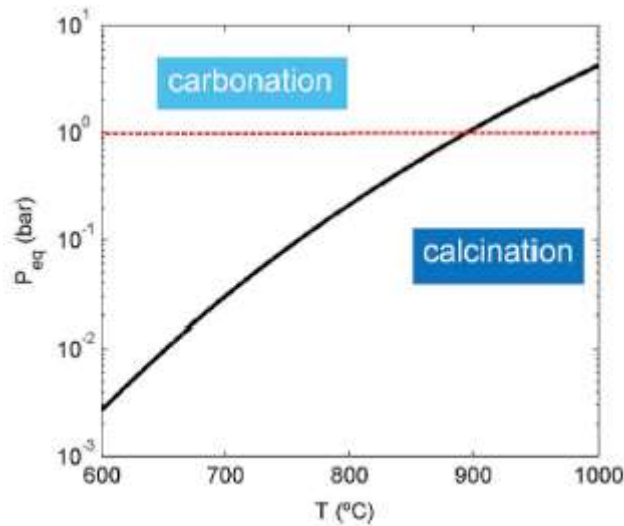


Figure 3-Equilibrium pressure as a function of the reaction temperature

The red dotted line represents the ambient pressure which, as it will be explained later, is relevant concerning our storage conditions.

In CCS applications [11], carbonator operates at low CO₂ partial pressure and high temperature, vice versa for the calciner. These conditions are the opposite ones with respect to ideal conditions that enhance the two reactions; moreover, they lead to a severe drop of CaO conversion with the number of cycles due to sintering and pores blocking of the regenerated CaO. Finally, CaO sulphation and the presence of ashes due to in-situ coal oxy-combustion contribute severely to a further drop in CaO conversion.

This is the reason why, for TCES applications (and in particular for SOCRATCES, as it will be explained later), chosen conditions are completely different, as we can see from the following table and graph:

CaI, process application	Typical conditions	
	Calcination	Carbonation
Post-combustion CO ₂ capture	950 °C high CO ₂ v/v atmosphere (oxycombustion) P = 1 atm	650 °C 15% v/v CO ₂ P = 1 atm
Thermochemical Energy Storage	~725 °C//950 °C (He or H ₂ O//CO ₂ atmosphere) P = 1 atm	~850 °C Pure CO ₂ P = 1-5 atm

Table 2 - Typical conditions for post-combustion CO₂ capture and solar energy storage [10]

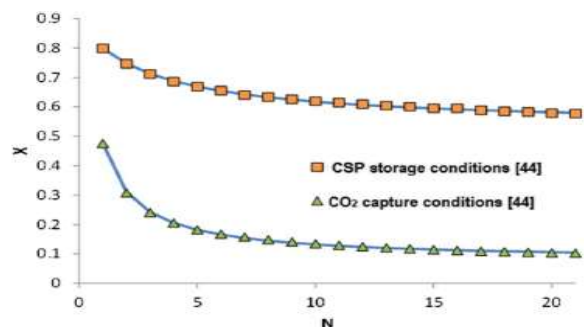


Figure 4 - CaO activity as a function of the number of cycles [19]

This change in operating conditions, as we can see from the graph on the right, leads to an improvement in CaO conversion and therefore a better performance of the plant.

As already mentioned, CaO reactivity (or activity or carrying capacity) is a fundamental and non-constant parameter, defined as the percentage mass change of a sample of CaO used in thermogravimetric analysis (TGA): in this experiment, a certain amount of calcium oxide undergoes a cycle of calcination/carbonation at the end of which the mass doesn't return to the initial value, but it shows a significant drop. This effect becomes more significant increasing the number of cycles. From a mathematical point of view, CaO reactivity can be expressed as the ratio between the number of moles that effectively takes part to the reaction to the total provided:

$$X = \frac{\text{moles CaO reacted}}{\text{moles CaO provided}} \quad (8)$$

One of the main obstacles to large-scale diffusion of the CaL process is represented by CaO deactivation, i.e. the reduction of its activity increasing the number of cycles, due to the fact that the reaction is not perfectly reversible: with the rising number of calcination/carbonation processes, CaO ability to react completely with CO₂ decreases, with a consequent inert mass of calcium oxide that increases more and more. This effect is due essentially to two de-activation mechanisms [3]:

- pore blockage of the CaO grains due to the formation of a layer of CaCO₃ on the surface during the carbonation. Since calcium carbonate has a higher molar volume than CaO, after a threshold value of thickness it is able to occlude the useful surface of calcium oxide and hinder thus its reaction with CO₂: from this moment, in fact, only solid particle diffusion of CO₃²⁻ and O²⁻ (counter-current with respect to the first one) is able to continue the reaction of carbonation. This is the reason why carbonation reaction can be subdivided into two phases: a first phase more rapid and kinetic-controlled, and a slower second one;
- sintering, a phenomenon linked to high temperature (for CaO around 533°C, about ½ of the melting temperature) and long residence time in the calciner and consisting in changes of pore shape, pore shrinkage and grain growth due to the phenomenon of coalescence.

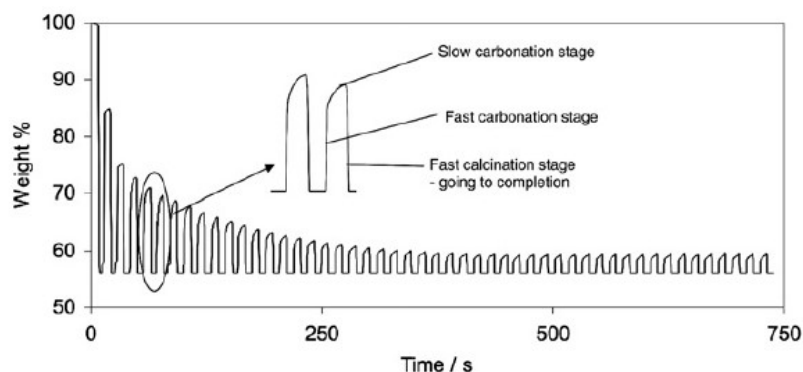


Figure 5 - Mass drop in repeated carbonation/calcination cycles [45]

With the graph above, where is represented the weight of the solid phase of both reactants and products with respect to the initial amount of CaCO_3 , is possible to notice that calcination tends to decrease the amount of solid phase (since there's the formation of CO_2 in gaseous phase), but the value of solid weight will be the same after all the calcinations because the conversion in CaO is complete. During a single carbonation, instead, it can be observed the first phase in which solid weight increase rapidly and the second one in which the increase is softer; moreover, the maximum value of the weight "recovered" from the carbonation tends to decrease asymptotically and this is linked to the already seen de-activation mechanisms.

However, it is possible to optimize the conditions in the calciner (and thus the CaO reactivity) by adding water (in form of steam) in it: in fact, even if steam acts as a catalyst for sintering process, its presence permits to have a lower value of CO_2 partial pressure and thus to work at lower temperatures (as it can be seen from Figure 4); lower operating temperatures mean also a lower contribution to sintering itself [2] and so there's a further improvement in reactivity. Moreover, last studies have found out that water sintering permits to open pore structures less susceptible to pore blockage, thus enhancing structure stability [3].

For the same purpose, instead of the steam it can be used helium (or other inert substances, like N_2): as for the steam, its presence decreases the partial pressure of CO_2 ; moreover, the use of He allows not to have any condensation or evaporation stages [2] and to have fast calcination at even lower temperatures, thanks to its high thermal conductivity and high CO_2 diffusivity in helium [10].

In both cases, water and helium are easily separable from CO_2 : for H_2O a condensation stage is sufficient, whereas to separate He it is needed a selective membrane.

For CaL process, since chemical reactions are involved, also kinetic has to be fully analysed; however, since in our case we are studying the plant in steady-state conditions, we can neglect the residence time in the reactors and so the kinetics itself. For parameters involved, values are taken from literature and a deep study is left to a second-stage analysis.

2.3 Description of the technology involved for the plant components

Now, with a general knowledge of the CaL process, it's possible to analyse how it can be integrated into a CSP plant by studying the technology involved.

A conceptual scheme of the system is represented in Figure 8:

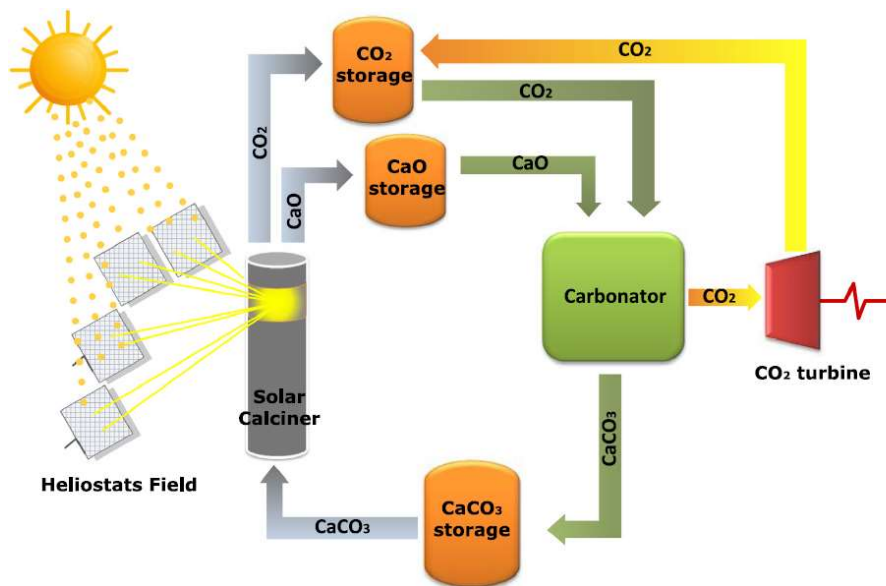


Figure 6 - Conceptual scheme of CSP/CaL plant [46]

As we can observe, solar heat is concentrated, conveyed onto the solar tower (which contains the calciner) and provided to the endothermic reaction, whereas heat from exothermic carbonation is provided to a suitable power plant in an indirect or direct way.

Another important thing that can be noticed is that this plant can be conceptually separated during the simulations into two defined parts in correspondence of the storages: the calciner side and the carbonator side. For all our simulations, by fixing some physical conditions, they can be treated as independent: while calciner side stores a certain amount of energy only if there is a certain solar radiation concentrated upon the solar tower surface, carbonator side can theoretically work at continuous power production at both rated power and maximum efficiency. As a consequence, instantaneous mass flows of calciner side will be higher than carbonator ones, but their integrals over a time period will be equal [2].

2.3.1 Solids conveying technology

The transport of solid particles can be performed generally in three ways: pneumatic, screw and tubular conveying. The latter two methods are reported briefly in the figure below.



Figure 7 - Alternative solids conveying systems: screw conveying (left) and tubular cable conveying (right) [3]

Pneumatic conveying is more mature and reliable than other ones, so it is the type of technology considered in SOCRATCES process. It consists in the transportation of solid particles by means of a gas flow, which carries it along a pipe up to a phase separator (e.g. a cyclone). The need for thermal exchange between solid and gas streams, the reduced particle size ($<300\ \mu\text{m}$) and the need for rapid transport are the reasons for which pneumatic conveying has been chosen for this project [3].

Pneumatic conveying exploits the concept of fluidization; according to different flow conditions, only two types of conveying are known: dilute and dense phase conveying.

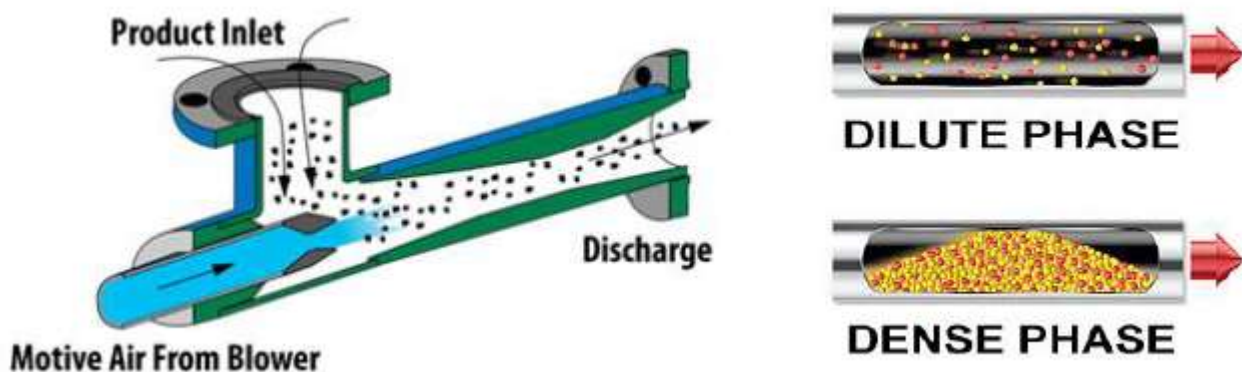


Figure 8 - Pneumatic conveying device and solid particles transportation phases [2]

For the first type of conveying, the material is transported in suspension in the flowing air along the pipeline with a minimum gas velocity between 13-15 m/s for most of the solid materials used worldwide. Almost any material can be conveyed in dilute phase, regardless of the particle size,

shape or density, but as already said, a relatively high velocity is required, with consequent high power requirements [3].

For the second type of conveying, solid particles are conveyed at low air velocity in a non-suspension mode; as a consequence, not all materials are naturally able of being conveyed in dense phase flow. Two modes of flow are known in this category [3]: moving bed flow, in which material is conveyed in dunes or as a pulsatile moving bed and that is suitable for materials in range 40-70 μm , and slug (or pug) flow, in which the material is conveyed in form of plugs separated by air gaps and suitable only for mono-sized materials with a good permeability to air. The main advantage for this mode is the lower energy consumption with respect to dilute phase conveying, so it is important to establish for each case if the material considered can be transported by means of low gas velocity conveying or not.

For all these reasons, dense phase conveying is the most suitable choice for SOCRATCES project; however, to avoid particle cohesion and thus a reduction of CaL efficiency, it is important to adopt some solutions, like sonoprocessing techniques, which exploit high-intensity acoustic fields (145-165 dB) to overcome adhesion forces and promote the gas-solid contact through a superposition of sound waves to the fluidizing flow, inducing large gas fluctuations and fluid recirculation within the bed [3].

2.3.2 Carbonator

In SOCRATCES project, the proposed technological solution for the carbonator is the pressurized Fluidized Bed Reactor (FBR), because its technical maturity and the advanced knowledge related to it permit to have a lower investment cost and a good reliability.

In this reactor, solid particles of CaO are conveyed by a gaseous stream of CO₂ (or, in alternative, helium); the products of the exothermic reaction are in different phases, so they are separated in a cyclone, from which they are obtained a gaseous flow of CO₂ (recirculated in the process) and a stream of solid particles that (as previously explained) are made of CaCO₃ on the external layer and CaO in the inner core. The excess of CO₂ at the inlet is necessary for two reasons: to control the temperature in the reactor by removing heat and to fluidize solid outlet streams ([2] and [12]). For this reason, one of the main operational parameters of this reactor is the fraction of CO₂ spent in the reaction (E, generally called CO₂ capture efficiency in CCS applications):

$$E = \frac{\text{mol } CO_2 \text{ reacted}}{\text{mol } CO_2 \text{ in}} = 1 - \frac{F_{CO_2,out}}{F_{CO_2,in}} \quad (9)$$

This parameter is dependent on other factors like the solid amount, the residence time in the reactor, the gas superficial velocity and the sorbent reactivity [3].

Some studies have focused on the optimal conditions to be set in the reactor. As we increase molar fraction (and thus partial pressure) of CO₂ (at constant total pressure), the reaction rate of the carbonation is enhanced; also an increase of the total pressure (at constant partial pressure of CO₂) leads to an improvement of the kinetic, but with a limit of 4000 torr (about 5,3 bar), over which the reaction rate starts to decrease:

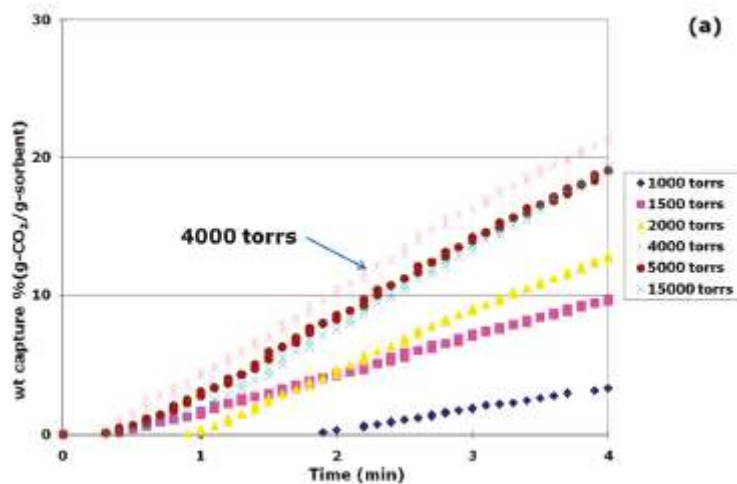


Figure 9-Effect of total pressure on the kinetic of carbonation [13]

This effect is explainable with a sort of “increase” in mass-transfer resistance, since by increasing the pressure (but fixing the amount of gas introduced) the CO₂ speed will decrease, with a consequent higher mass-transfer resistance that obstacles the reaction between carbon dioxide and CaO [13].

Finally, from Le Châtelier principle for exothermic reaction with decreasing number of moles (and thus increasing order), reaction rate is enhanced by lowering the temperature; however, in this project we want the carbonator temperature as high as possible in order to have high-quality heat supplied to the power cycle and thus improve its efficiency, a sort of compromise between the two opposite effects [2].

2.3.3 Calciner

For the calciner, as already mentioned, operating conditions are very different: in fact, lower T are needed in order to have a sorbent as little-sintered as possible upon calcination [3] and, by some considerations about chemical equilibrium, it means lower CO₂ partial pressure. Low temperatures (below 700°C) are requested mainly for three reasons [2]:

- to have better performances in terms of CaO activity;
- to achieve a technical feasibility of the system by using a mature, reliable and thus not expensive solar central receiver (since there aren't high temperatures to be sustained);
- to have lower convective and radiative heat losses compared to traditional CSP plants.

Since we want a low partial pressure of carbon dioxide in the reactor but we desire a pure CO₂ stream as a product, there are mainly two options [3]:

- calcination under reduced pressure in 100% CO₂ atmosphere, which nevertheless requires a strong vacuum atmosphere to be achieved and, from a point of view of kinetics, makes the calcination slower;
- dilution with steam, which not only acts as a solid reactant carrier, but also as a heat transfer medium (lowering the required temperature) and, as already said, as an enhancer of CaO activity.

This project adopts for the calciner the already developed Fast Calcination Technology (or Catalytic Flash Calcination (CFC) introduced by CALIX) with an entrained flow reactor with superheated steam dilution. A scheme of the reactor is reported in Figure 10.

After the calcination, the products pass through a cyclone (to separate solids)

and a condenser (to separate steam from CO₂) and then sent to the storages. As easily understandable, the combustors that are present in the image are not present in our case, since thermal power is supplied by solar radiation.

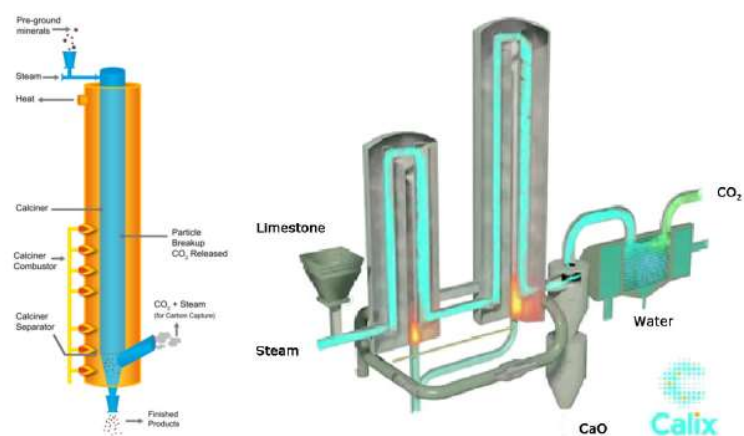


Figure 10 - Catalytic Flash Calcination by Calix [3] [47]

Finally, it is very important to have an efficient heat recovery network, since CaCO_3 is extracted from storage at ambient temperature whereas products are released at the calcination temperatures, in order to have a smaller amount of solar energy involved in the heating of the reactants up to the desired temperature and a bigger one involved in the reaction itself (and thus an increase of the efficiency) [2].

2.3.4 Storages

Concerning the solid compounds storage, storage conditions are the same of the external environment; for this purpose, since SOCRATCES pilot plant is going to be installed in Seville (Spain), they are chosen to be realistic with respect to the location: 20°C and 1 bar. Anyway, a precise choice has been made in this study: if heat recovery network design presents some difficulties to completely cool down the solid products (both of calcination and carbonation), they are sent to storages at higher temperatures; this aspect permits to have a lower preheating and a higher amount of sensible heat stored to be used in the next carbonation/calcination [2], but requires a certain degree of attention about insulation of the storages to avoid thermal losses.

For CO_2 instead, things are different and quite complex: as a gas, a kilogram of carbon dioxide will occupy a volume much higher than a solid compound, so in terms of volumetric energy density that can be stored there is an issue. To solve it, CO_2 has to be maintained at high pressures and low temperatures.

Two main alternatives are taken into account to compress CO_2 up to the high pressures requested ([3] and [2]):

- compressions with intercooling stages up to subcritical pressures (about 20 bar) + cooling and liquefaction down to cryogenic temperatures (and eventually a pumping);
- compressions with intercooling stages up to supercritical pressures (about 75 bar) + cooling down to about 25°C (near ambient temperature) without necessity of a refrigeration cycle (with a saving in energy consumption, capital and O&M costs).

For our purpose, in order to make this technology competitive in the market, the most interesting choice is the second one.

Another aspect which is interesting to be evaluated is what parameters influence most the storage capacity, as we can observe from the following graphs:

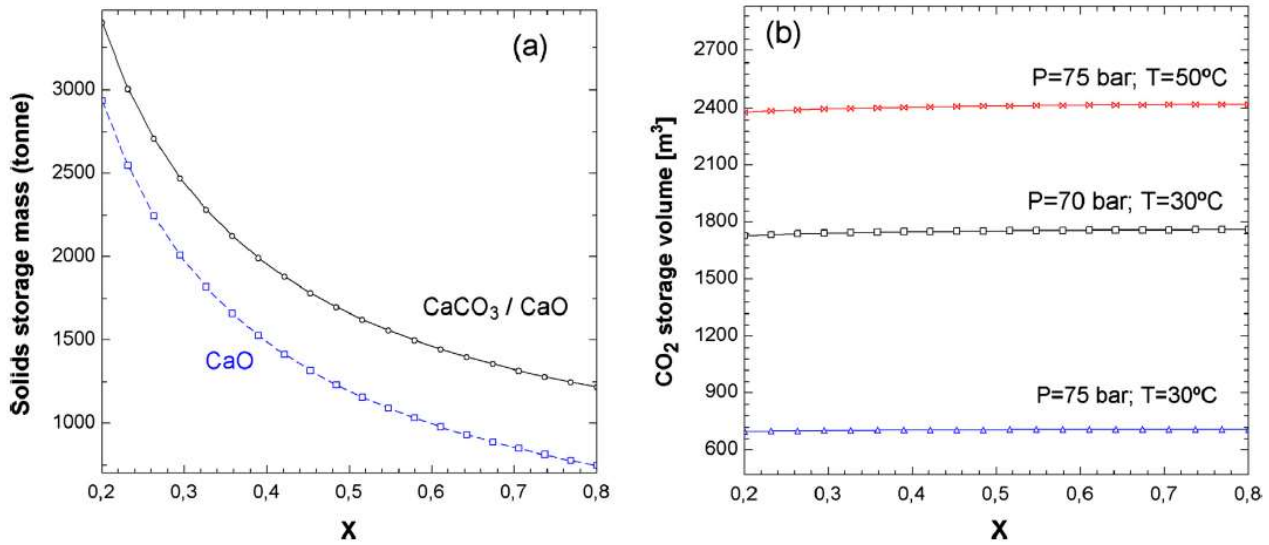


Figure 11 - (a) Solids storage mass as a function of average CaO conversion. (b) CO₂ storage volume as a function of average CaO conversion for several storage conditions. [9]

We can notice that, while increasing the average CaO conversion allows for an important reduction of the solid compounds storage volumes, the same cannot be told about CO₂ storage, which is instead more sensible to gas density (and thus storage temperature and pressure) [9].

2.3.5 Gas turbine technology

This kind of technology is well known, reliable and fully developed. For simplicity and compactness, simple thermal cycles without reheating or intercooling stages would be the best choices (even if they represent an improvement for thermal efficiency and for reduction of exergy losses ([14] [15])); however, while the former solution is not applicable in our case (because of unavoidable mixing between gases), the latter one permits to have a lower compression work in case of high ambient temperatures, thus enhancing the efficiency [3].

Conventionally, compact machines are used in the power cycle, including both compressor, fuel-fired combustor and turbine for the power fluid, since they represent a saving in terms of costs and a gain in performances [3]; in our work, however, gas compressor and turbine are decoupled, whereas the role of the intercooling stage has to be fully analysed.

A further solution is proposed for gas compressor in the carbonator side:

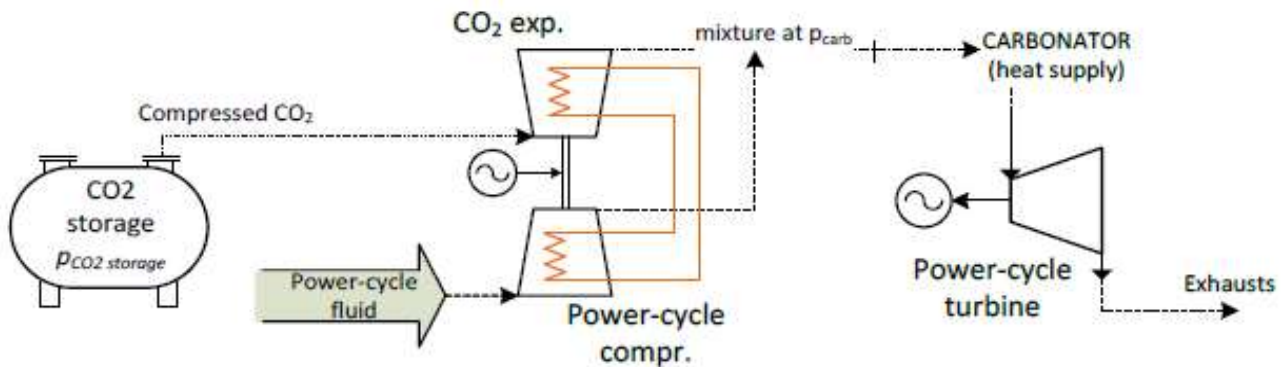


Figure 12 - Compressor and turbines arrangement in carbonator side [3]

Since a decompression of CO₂ from storage to cycle conditions is needed in any case, a coupling of this expansion turbine with the power-cycle compressor not only permits to cover part (or all) of the energy needed by the latter one, but also to have an additional intercooling stage installed, since carbon dioxide after expansion is at very low temperatures and thus helps cooling the compressed CO₂ [3].

2.3.6 Heat exchangers

Heat exchangers used in the recovery networks are essentially of three types, according to the type of fluids involved:

- for gas-to-gas heat exchange, closed configuration is the only one possible, to avoid mixing. Several type of heat exchangers have been fully developed and studied for this case: shell-and-tube, plate, plate-and-shell, primary surface and spiral plate;

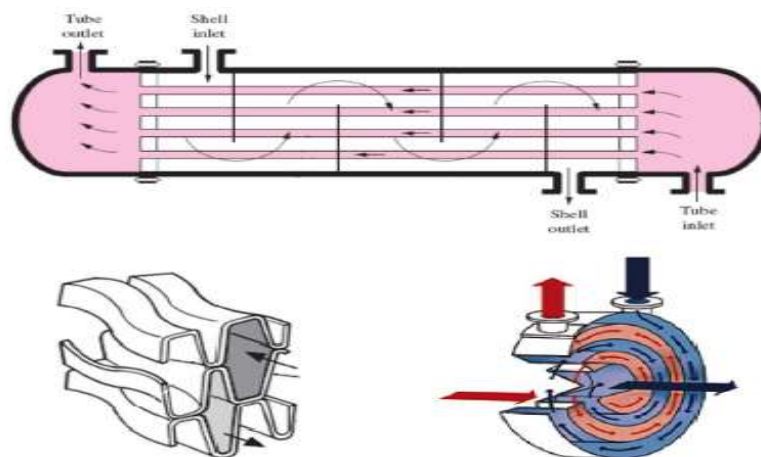


Figure 13-Different configurations of gas-to-gas heat exchangers [2]

- for gas-to-solid heat exchange, both closed and open configuration are possible. The best choice for direct (open) configuration is the cyclone heat exchanger: particles, inserted by means of particle diffuser to improve radial dispersion, move in a “counter-flow” with respect to the gas, which is inserted the upper part into the chamber in downward axial direction, making a strong swirl within it and then flowing back from the top (and that’s the difference from the conventional cyclone separators) [3].

For indirect (closed) configuration instead, a good choice is represented by an innovative plate exchanger system for heating or cooling bulk solids, by means of a fluid without direct contact; while solids descend by gravity, they are cooled or heated by the gas passing between the plates in counter-current [2];

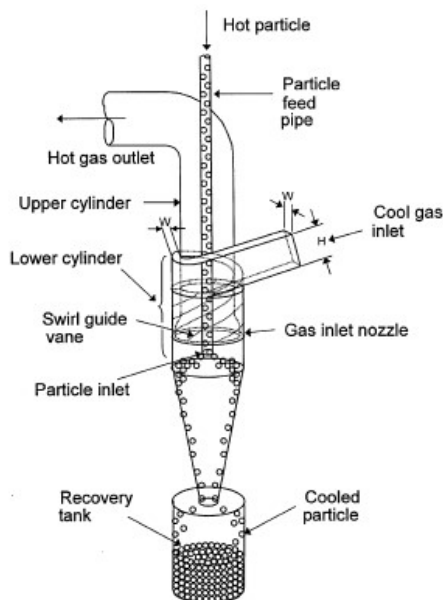


Figure 14 - Direct gas-gas heat exchanger [48]

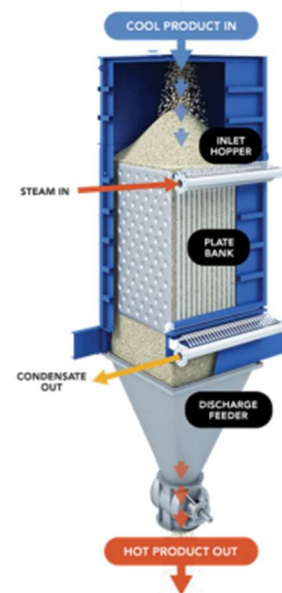


Figure 15 - Indirect gas-solid heat exchanger [49]

- for solid-to-solid heat exchange, technology is instead not fully developed. The most feasible solution seems to be the one with two indirect solid-gas heat exchangers in parallel, where the same heat transfer fluid is recirculated through both of them, removing heat from the first solid bulk and supplying it to the other one; this solution has to be fully analysed in terms of thermal properties of the heat transfer medium. More complex alternatives are linked to the fluidization of the solid bulks in heat exchangers and their usage as normal fluids, or the exchange of heat between solids by direct conduction through a solid wall [3]; however, they are too much difficult to be implemented, so they aren’t taken under investigation in our project.

2.4 SOCRATCES goals to achieve

SOCRATCES project, after the preliminary studies and investigations about the best theoretical conditions and components, forecasts an experimental phase, subdivided into many levels [16]:

- firstly, a 10-kW prototype will be constructed to identify and solve the points of weakness before the scaling up of the project; moreover, this step forecasts the solar integration with the calciner, the control of the systems and the material transport. The planned period was 2017-2020, even if further updates fixed its start at the beginning of 2018;
- after that a 1 MW pilot plant will be built in Seville, starting from advances obtained with previous level, to obtain the best working conditions and solve the last scaling challenges (period 2020-2023);
- finally, the first, demonstration-aiming and commercial-size plant will be realised (period 2023-2025).

Anyway, during this period all the compounds and components involved will be fully studied in order to obtain an optimized and performing power plant.

The practical goals of the project are represented in the following figure:

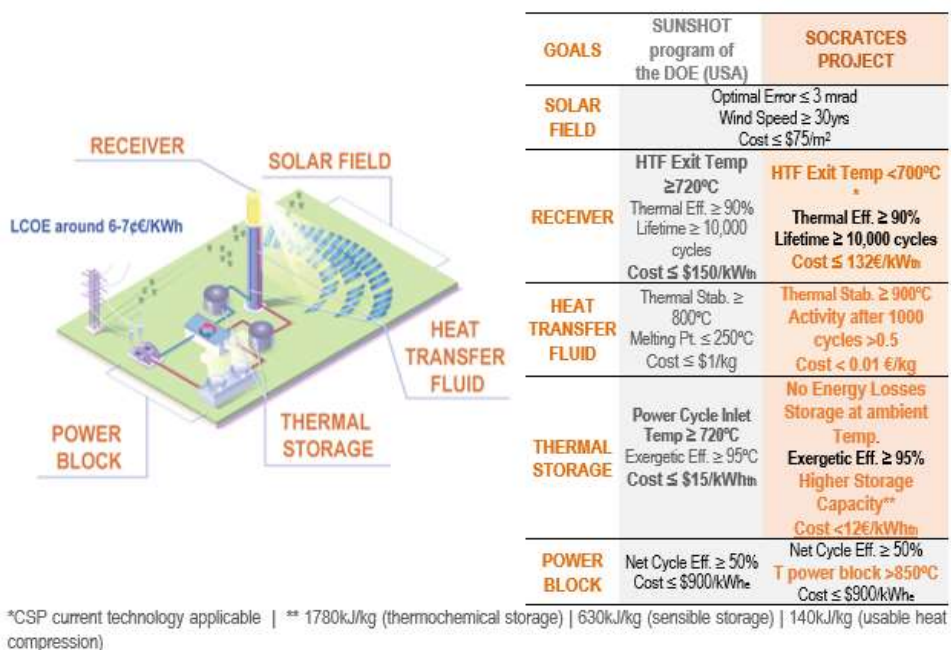


Figure 16 - SOCRATCES goals [16]

After the complete reaction of CaCO_3 in the calciner, the products (CO_2 and CaO) pass through a network of heat exchangers to preheat solid reactants entering the calciner; moreover, carbon dioxide is stored under pressure (whereas solids are stored at ambient conditions), so it has to undergo a multi-stage intercooled compression (even if in the scheme it is represented only one compressor, in real conditions, as already explained, it is better performing to have this type of compression). A suitable separation unit must be installed to separate steam (or He) that are presents in reactor atmosphere for optimal working conditions [2].

For the carbonator side instead, compressed CO_2 is mixed with compressed air (at carbonator pressure) and preheated by reaction products before entering the reactor; also CaO exiting from storage is preheated through a heat recovery from carbonation products [10]. In this scheme, CO_2 entering the carbonator is assumed to react completely with CaO , so there isn't any excess of carbon dioxide in this ideal situation; therefore, a pure air stream is released from carbonator, provided to the power turbine to produce electricity and then released directly to the atmosphere. However, at a given temperature, carbonation will proceed until CO_2 concentration reaches a limit threshold, corresponding to the point of thermodynamic equilibrium of carbonation [10] over which it's not possible for CO_2 to react with CaO and thus it's unavoidable to have a percentage of carbon dioxide in the gas vented to the atmosphere; moreover, since ideal thermodynamic equilibrium isn't reached in real conditions, the CO_2 concentration will be even higher than this theoretical limit. Since this project started with the aim of free CO_2 power production, open Brayton cycle is not a suitable choice.

To overcome this situation, an alternative is represented by a regenerative CO_2 closed Brayton cycle whose scheme was realized by Chacartegui et al. ([19] and [12]). A conceptual scheme, realized by Ortiz et al., is represented in the figure below.

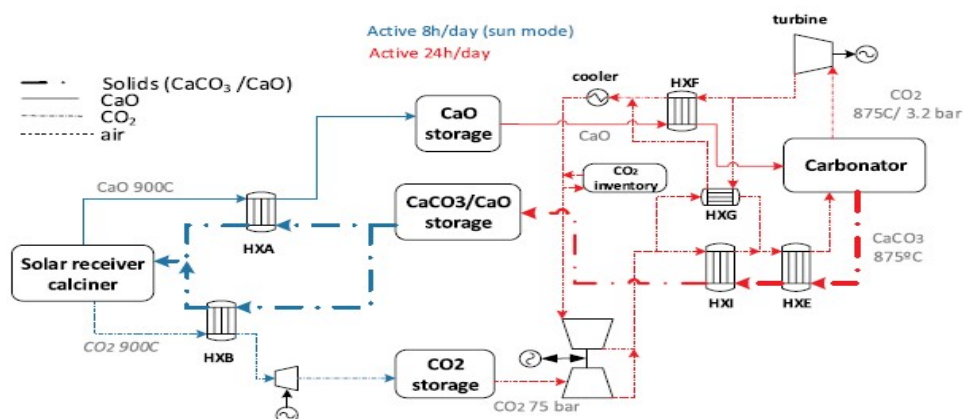


Figure 18 - CSP-CaL indirect integration with CO_2 closed cycle [10]

In the former of these works, a first type of scheme was analysed particularly concerning the optimal pressure ratio (PR) of the carbonator to the turbine outlet; as a solution for the main problem affecting the previous plant type, CO₂ enters the carbonator in excess with respect to the stoichiometric quantity and the amount not reacted acts as a heat carrier fluid that is supplied to the power turbine and then thermally regenerated (through the heat recovery system) and compressed, before being mixed to carbon dioxide coming from the storage [10]. This study finds out that the efficiency reaches its maximum at PR=3,2 and this is independent from the CaO conversion value:

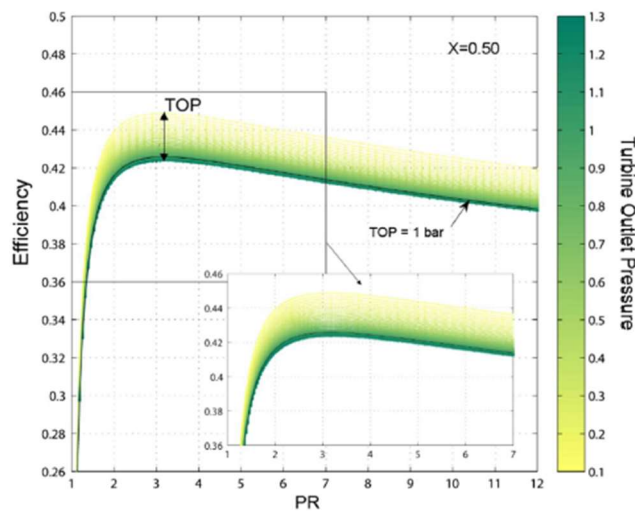


Figure 19 - Plant efficiency as a function of pressure ratio (PR) and turbine outlet pressure (TOP) for fixed CaO conversion ($X=0,5$) [19]

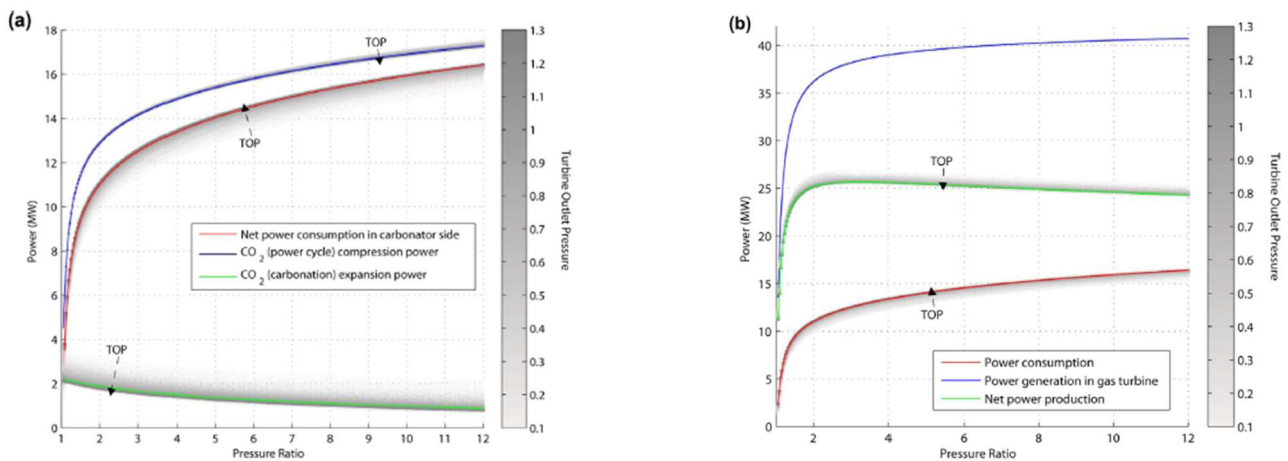


Figure 20 - Effect of PR on power production and consumptions [19]

In fact, higher PRs mean lower temperatures at the outlet of the turbine and thus lower temperatures of CaO particles entering the carbonator, whereas lower PRs lead to higher CO₂ flow

rates needed in the power cycle; finally, lower absolute pressures in the carbonator lead to lower net consumption for turbine/compressor complex linked to CO₂ storage [10].

In the latter work [12], instead, the focus was upon the improvement of the heat exchange network: starting from the configuration utilized for open cycle (as in Figure 19) with adaptations coming from the use of a closed Brayton cycle, an enhancement of the global efficiency of the plant is obtained by an improvement of the heat recover [10].

3.2 Indirect integration

Regarding the indirect integration, many studies have been carried out to find the best integration cycle and the optimal conditions related to it; a general scheme is provided in the figure below.

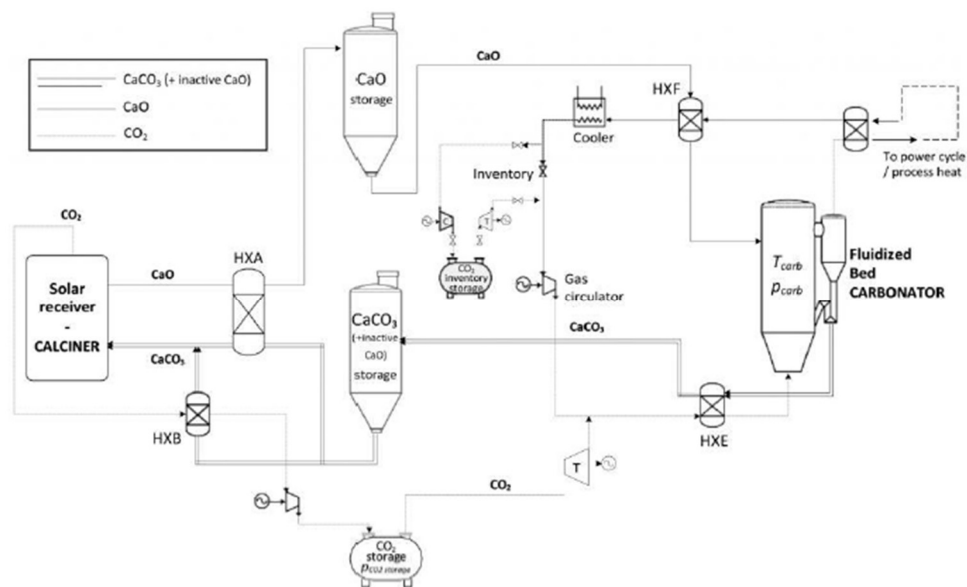


Figure 21 - Indirect integration scheme [2]

In this configuration, the power block and the carbonator side are not anymore directly integrated, since they only exchange thermal power through a heat exchanger, exactly as a heat recovery made for the reactants preheating [2].

As already said, scientific literature has already focused upon this argument: particularly, Ortiz et al. [9] explored many different cycles to find out the best choice, and then they compared them with the performances obtained with the direct integration. Power cycles under investigation are a sub-

critical Rankine cycle with reheat, a recompression supercritical CO₂ (sCO₂) Brayton cycle and a Combined Cycle (CC). The results obtained are reported in the following graph:

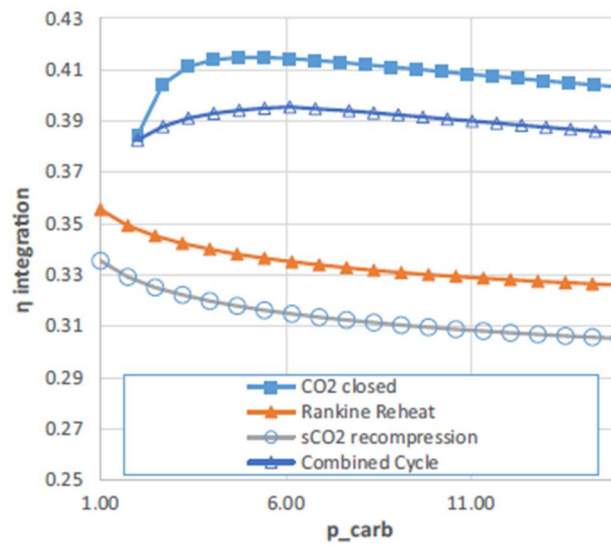


Figure 22 - Comparison between different indirect integrations performances [9]

As we can observe, the CO₂ closed cycle direct integration yields the best efficiency results. Moreover, only indirect integrations allow to operate under atmospheric pressure in the carbonator, being the efficiency hampered in this integration as the carbonator pressure is increased; the opposite trend is instead observed in the CO₂ closed and CC power cycles [9], where the global efficiency is enhanced with increasing carbonator pressure up to a certain optimum value (around 4.2 bar for the CO₂ closed cycle and 5.1 bar for the CC, both with atmospheric turbine outlet pressure) [9]. Finally, even if the sCO₂ recompression cycle could be potentially attractive from a thermodynamic point of view, the conservative values used for the turbomachinery efficiencies represent an obstacle for reaching very high global efficiencies [9].

Finally, another type of scheme analysed that mixes both direct and indirect integration is the one considering high temperature solid storage [20]. An integration scheme is reported below.

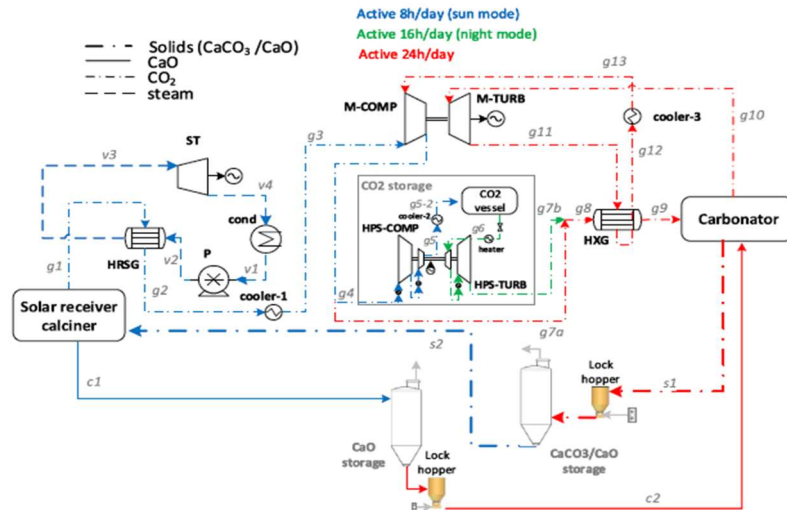


Figure 23 - Integration with high energy storages [20]

While in the carbonator side the power cycle utilized is a regenerative (direct) CO₂ Brayton cycle, in the calciner side CaO is sent directly at high temperature into the storage, while carbon dioxide produced in the calciner releases part of its sensible heat to solid CaCO₃ preheater and to a heat recovery steam generator (HRSG) that supplies a Rankine cycle (indirect integration). In this way, it is also possible to avoid the solid-solid heat exchange, that isn't trivial as already said.

Two last considerations have to be done about CaL integration [2]:

- for all the power cycles analysed (except for open air/CO₂ cycle, since there is not recirculation), a CO₂ inventory storage complex (with turbine and compressor) has to be included, in order to modify the amount of carbon dioxide recirculated during the transient phase of the carbonator side. Anyway, since in our study we assume steady-state conditions for our simulations, we can ignore its presence;
- as previously said, calciner and carbonator side can be treated and simulated separately, and this aspect finds confirmation in the fact that (in first approximation) calciner side layout isn't influenced by the power cycle integration.

With all these considerations about general CSP-CaL integration with power cycle, we can now introduce the type of power cycle considered in this work, i.e. Organic Rankine Cycle (ORC).

3.3 Organic Rankine Cycle (ORC)

The Organic Rankine Cycle (ORC) is a type of Rankine power cycle that exploits a fluid with a molecular weight higher than the water's one and with a liquid-vapor phase change (or boiling point) occurring at a lower temperature than the water-steam phase change. The choice of this type of plant is thus useful for recovering low-grade heat (in general, in many applications it starts being useful at $T < 370$ °C [21]); consequently, in our case, where carbonator reaches high temperatures (so a diametrically opposed situation with respect to the usual one for ORCs), it could be interesting to analyse their integration with CaL process because of the favourable thermal properties of these fluids and the advantages in terms of performance at reduced power loads given by the machineries [2].

The organic fluids involved present some characteristics that have to be carefully analysed for the specific choice ([22] and [23]):

- T-s diagram close to isentropic one. In fact, the main difference between these organic fluids and water (used in Steam Rankine Cycle or SRC) is their behaviour during the expansion from saturated state through a turbine at low and moderate temperature: with most of organic fluids, an isentropic expansion from saturated vapor results in superheated vapor, rather than a two-phase mixture as with water, avoiding complications to turbine and cycle design. This is due to the slope of the vapor saturation curve of the fluid in this region, i.e. positive for organic fluids, negative for water and infinite for isentropic fluids; consequently, it is possible to subdivide medium for Rankine cycles into three categories (dry, wet and isentropic), as it can be observed from the following figure:

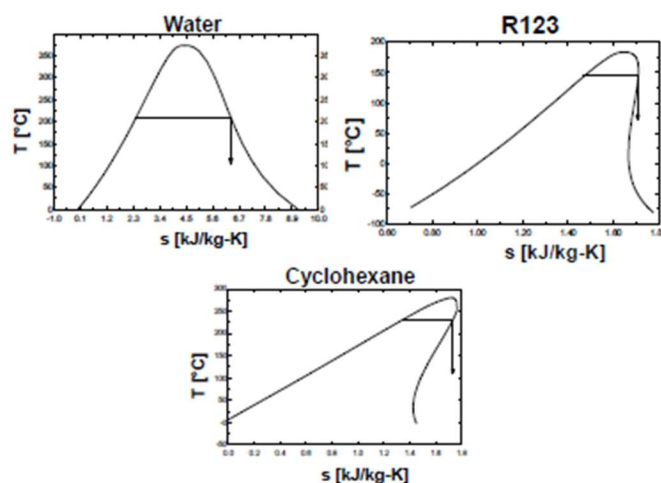


Figure 24 - Examples respectively of a wet, isentropic and dry fluid [22]

In the following table, some of the fluids analysed in the literature and their classification are reported:

Fluid	Tcrit [°C]	Pcrit [kPa]	Type
Water	374.0	22064	wet
n-pentane	196.5	3364	dry
HFE 7100	195.3	2229	dry
Cyclohexane	280.5	4075	dry
Toluene	318.6	4126	dry
R245fa	154.1	3639	isentropic
n-dodecane	385.0	1817	dry
R123	183.7	3668	isentropic
Isobutane	134.7	3640	wet

Table 3 - Classification of working fluids [22]

- high molecular weight: the higher is its value, the more positive is the slope of the saturation curve (a positive effect);
- non-corrosivity and low toxicity;
- low flammability;
- low cost;
- low Ozone Depletion Potential (ODP) and Global Warming Potential (GWP): ODP is calculated as the ratio of ozone destruction per unit mass of released gas, whereas GWP is a factor that estimates how much the mass of a chemical will increase the global warming, over a period of 100 years [22];
- low viscosity;
- compatible with materials;
- value of specific heat of liquid similar to the one of vapor.

Fluids reported in the table are some examples of those involved in ORC plants, whereas other media exploited can be found in literature ([24], [25] and [23]).

A typical scheme of an ORC plant is represented in the figure below:

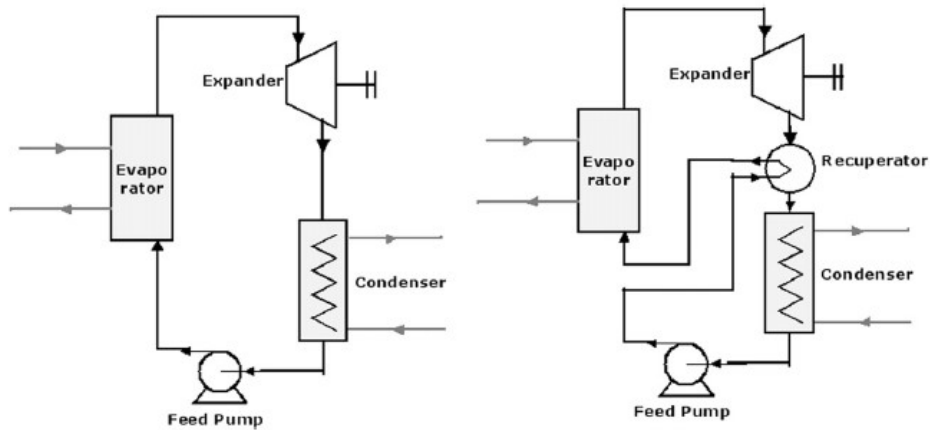


Figure 25-Typical ORC plant scheme without and with recuperator [25]

Components involved are the ones typically exploited in SRC, with the addition of a regenerator (or recuperator) to recover the heat of the superheated vapor exiting from the turbine to preheat the fluid before entering the evaporator. As we will see in the next chapters, in our analysis we will start from temperatures obtained with optimization done in previous works but without a starting heat exchangers network, and our purpose will be exactly to find it and to discover whether a recuperator is necessary or not.

Moreover, similarly to “traditional” Rankine cycles, ORCs can be subdivided into supercritical and subcritical cycles, depending on whether maximum pressure is higher or not than critical value for that specific organic fluid; in terms of plant scheme, in a supercritical cycle the evaporator is substituted by a generic heating stage due to the absence of a defined phase change step. T-s and T- ϕ diagrams of both cases are reported in the figure below, where a regenerator is placed, and yellow and blue lines represent respectively a hot source temperature trend example and a cold sink one; it is interesting to notice that in the supercritical case is possible to obtain a heating curve that matches the variable temperature heat source, reducing thus the overall logarithmic temperature mean difference and the efficiency losses due to heat exchange with finite temperature differences:

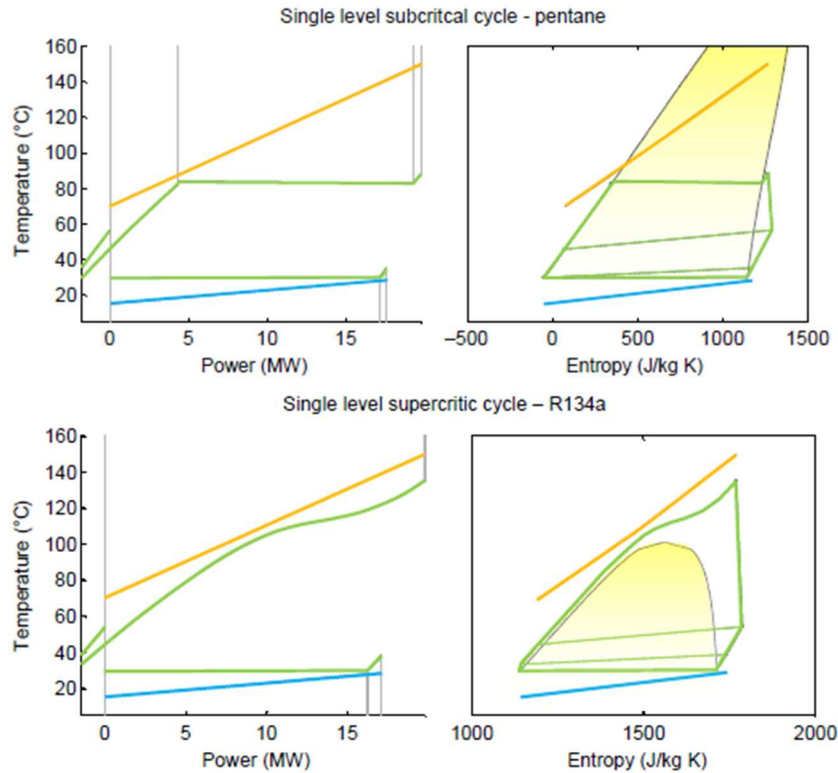


Figure 26-Subcritical and supercritical cycles [50]

In this study it will be analysed the supercritical cycle of benzene (C_6H_6), an isentropic organic fluid. Since we utilize results obtained in simulations and analyses performed in a previous thesis [2], we have to briefly introduce some assumptions made about cycle parameters:

- condensing pressure is assumed to be at a value lower than atmospheric pressure because, even if is safer to have a higher value to avoid air infiltrations, in terms of thermodynamic efficiencies it is more interesting to condensate under vacuum conditions. However, a lower boundary value of 0,1 bar is set for machinery limits;
- temperature has a lower limit value of 35°C (that is reached in condensation stage) for a thermal exchange purpose (since $T_{amb}=20^{\circ}C$ and $\Delta T_{pinch\ point}$ is assumed equal to 15°C, as explained later);
- constant values for efficiencies of all the machineries involved (pump, electric, turbine) have been imposed (we don't report here the values involved since we will work on results of the simulations, so assumptions about how they're obtained are not of interest);
- a vapor fraction minimum limit for the entire expansion has been set to a value of 0.85, in order not to have an excessive formation of condensate in the turbine;

- maximum temperature and pressure at the turbine inlet are set in order to overcome the maximum sustainable conditions, so, upper limits of these quantities are set respectively to 510°C and 110 bar.

With all these introductory aspects that have been fully exposed, we can now start explaining the analysis performed in this work.

4 Heat exchanger network design

The work of this master's degree thesis starts from the results of a previous thesis written by Tesio et al. [2]: starting from temperatures that he obtained in the optimization of the ORC indirect integration (where the power cycle presented the features already explained in previous chapters), the first step is to design the corresponding heat exchanger network. In order to understand how these temperatures are obtained, let's firstly introduce a brief explanation of the optimization algorithm involved in the previous work.

4.1 Optimization of the ORC integration

To introduce the algorithm utilized in the optimization process, it can be useful to analyse a flowchart taken from that thesis.

Firstly, thermodynamic cycle has been optimized separately from the rest of the plant because, even if from a theoretical point of view it is more correct to optimize both the carbonator side and the ORC cycle together, it is more practical and computationally simpler to optimize firstly the power cycle and then to insert temperatures obtained here into the second step of the optimization where carbonator side is optimized. From this preliminary step, streams data (temperature, flowrate, pressure, specific heat capacity through linear interpolation from Aspen dataset) are obtained from single variable (i.e. the evaporation pressure) optimization, performed with the quadratic approximation method. At

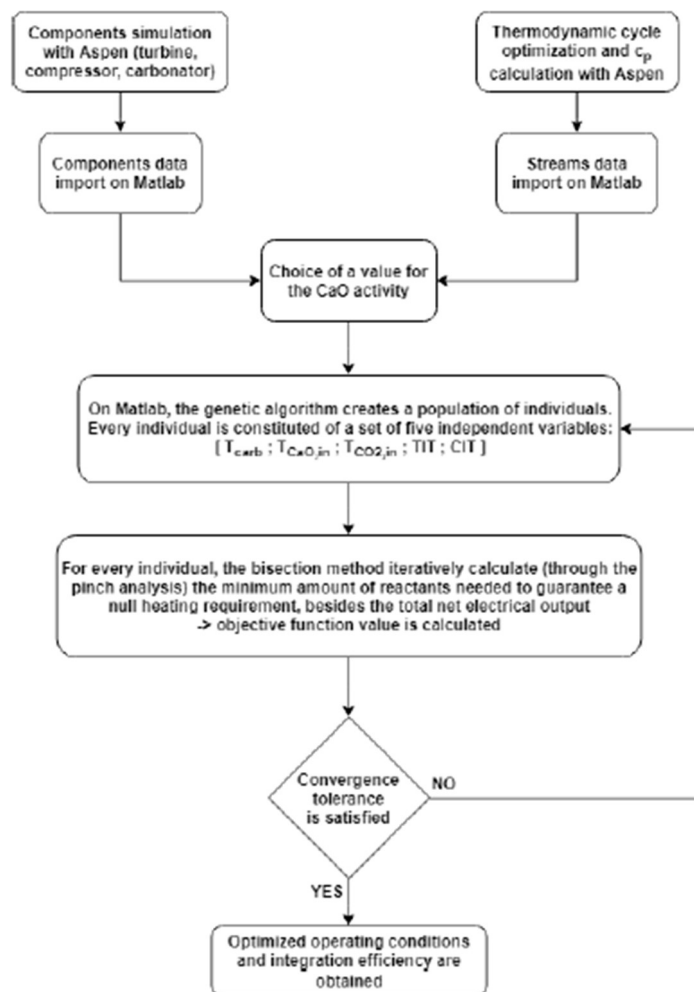


Figure 27 - Optimization algorithm [2]

the same time, also operating conditions of some components important for the plant (as the excess index and both the turbine and compressor outlet temperatures, TOT and COT respectively) have been obtained from Aspen simulations, but since these are dependent variables for the optimization (so they're obtained from the values of the independent ones), they are imported on MATLAB to be used in the next step of the algorithm.

After having chosen a value for the CaO activity (an independent variable for the process, treated as discrete for the optimization for practical reasons, since a change in its value needs a new run of the algorithm), the genetic algorithm involved in the optimization process selects a population of individuals whose elements are a set of values for five independent variables (all treated as continuous in the optimization process, except for the carbonator temperature that has discrete values for practical reasons): the carbonator temperature, the CO₂ inlet temperature, the CaO inlet temperature, the compressor inlet temperature (CIT) and the turbine inlet temperature (TIT). From these values, all the other dependent variables (intermediate temperatures, pressures and flowrates) are obtained through calculations.

For every set of values of independent variables (and dependent ones related to them), bisection method is used to iteratively calculate the minimum CaO flowrate in order to guarantee a null heating requirement from the external environment (through pinch analysis), having firstly obtained values for specific heat capacities from both mathematical correlations and Aspen dataset; by using the CaO flowrate obtained, the net electrical power per unit of CaO mass flow is evaluated, that is the objective function to be maximized. In other words, the aim of the process is to obtain the maximum electrical power produced with the lowest consumption of reactants involved [2]. The algorithm stops when the convergence tolerance is reached, and the objective function is maximized.

In the following tables, values obtained for ORCs integration are reported.

	BENZENE		CYCLOHEXANE		CYCLOPENTANE		ETHANOL		TOLUENE	
	P [bar]	T [°C]								
1	0,198	35	0,2009	35	0,619	35	0,138	35	0,1	45,25
2	112,25	40,20	112,25	40,93	59	38,23	112,25	38,9	112,25	50,39
3	110	428	110	365	57,82	270	110	370	110	420
4	0,202	223,8	0,205	201,4	0,631	116,6	0,14	98,8	0,102	216,2
\dot{m}_{ORC}	3,724 [kg/s]		4,614 [kg/s]		6,466 [kg/s]		2,404 [kg/s]		4,268 [kg/s]	
η_{cycle}	27,46%		24,19%		22,81%		28,91%		25,86%	
$\dot{W}_{s,turb}$	1095 [kW]		1121 [kW]		1100 [kW]		1077 [kW]		1107 [kW]	
$\dot{W}_{s,pump}$	64,5 [kW]		90,2 [kW]		68,9 [kW]		46,3 [kW]		75,6 [kW]	
Gain %	9,05%		5,04%		4,78%		3,29%		5,04%	

Table 4 - Optimized ORC cycle main parameters [2]

	X [-]	Storage turbine power [kW _e]	Compressor power [kW _e]	Conveying power [kW _e]	Rejection power [kW _e]	Total auxiliaries consumption [kW _e]	Total plant net power [kW _e]
BENZENE	0,2	309	0,45	106	12,8	119	1181
	0,3	308	7,51	73	13,3	86	1205
	0,4	307	12,61	56	13,2	70	1216
	0,5	305	16,48	46	12,6	59	1221
CYCLOHEXANE	0,2	333	0,08	114	15,0	129	1194
	0,3	331	7,86	78	14,9	93	1220
	0,4	330	13,81	61	15,1	76	1231
	0,5	328	16,61	50	14,5	64	1238
CYCLOPENTANE	0,2	430	0,12	147	20,6	168	1249
	0,3	427	9,09	101	21,3	122	1283
	0,4	427	14,52	78	21,4	100	1300
	0,5	424	18,5	64	21,1	85	1308
ETHANOL	0,2	378	0,1	129	17,2	147	1220
	0,3	375	8,43	89	18,0	107	1249
	0,4	375	13,76	69	17,4	86	1264
	0,5	373	16,72	57	17,8	74	1271
TOLUENE	0,2	325	0,08	111	13,7	125	1190
	0,3	322	7,88	76	13,6	90	1215
	0,4	321	13,91	59	13,2	72	1226
	0,5	320	17,09	49	13,8	62	1231

	INDEPENDENT VARIABLES						DEPENDENT VARIABLES				FLOWRATES					
	X [-]	T _{amb} [°C]	T _{CO₂in} [°C]	T _{CO₂out} [°C]	TIT [°C]	CIT [°C]	COT [°C]	TOT [°C]	T _{CO₂out} [°C]	Excess index [-]	m _{CO₂0} [kg/s]	m _{CO₂static} [kg/s]	m _{CO₂rec} [kg/s]	m _{CO₂unr} [kg/s]	m _{CO₂} [kg/s]	η _{carb} [%]
BENZENE	0,2	875	397	44	649	47	58	293	280	1,059	4,91	0,77	0,046	3,93	1,75	37,83
	0,3	875	310	47	650	158	172	294	242	1,735	3,25	0,77	0,564	2,28	1,74	38,84
	0,4	875	310	49	650	126	139	294	205	2,338	2,44	0,77	1,024	1,46	1,74	39,37
	0,5	875	310	81	650	116	129	294	188	2,803	1,94	0,76	1,371	0,97	1,73	39,65
CYCLOHEXANE	0,2	875	368	174	650	183	197	294	293	1,007	5,29	0,83	0,006	4,23	1,89	35,53
	0,3	875	310	57	650	138	151	294	233	1,751	3,49	0,82	0,619	2,45	1,87	36,61
	0,4	875	310	62	650	125	138	294	204	2,367	2,62	0,82	1,124	1,57	1,87	37,13
	0,5	875	310	98	650	82	94	294	164	2,851	2,08	0,82	1,514	1,04	1,86	37,39
CYCLOPENTANE	0,2	875	368	176	650	146	159	294	293	1,009	6,82	1,07	0,009	5,45	2,43	28,83
	0,3	875	311	51	650	99	112	294	216	1,743	4,51	1,06	0,791	3,16	2,42	29,81
	0,4	875	311	51	650	56	68	294	164	2,344	3,38	1,06	1,429	2,03	2,42	30,34
	0,5	875	310	53	650	55	67	294	150	2,726	2,69	1,06	1,825	1,34	2,4	30,55
ETHANOL	0,2	875	368	176	650	137	150	294	292	1,009	6,00	0,94	0,008	4,80	2,14	32,00
	0,3	875	311	47	650	122	135	294	226	1,738	3,96	0,94	0,690	2,78	2,13	33,04
	0,4	875	311	47	650	84	96	294	181	2,336	2,97	0,93	1,248	1,79	2,12	33,54
	0,5	875	311	47	650	67	79	294	158	2,712	2,36	0,93	1,591	1,18	2,11	33,84
TOLUENE	0,2	875	368	174	650	184	199	294	293	1,007	5,15	0,81	0,005	4,12	1,84	36,37
	0,3	875	310	65	650	142	156	294	234	1,765	3,40	0,80	0,614	2,39	1,82	37,42
	0,4	875	310	97	650	114	127	294	195	2,452	2,55	0,80	1,163	1,53	1,82	37,95
	0,5	875	310	118	650	90	102	294	168	2,912	2,03	0,80	1,523	1,01	1,81	38,21

Table 5 - Main optimized parameters of the plant [2]

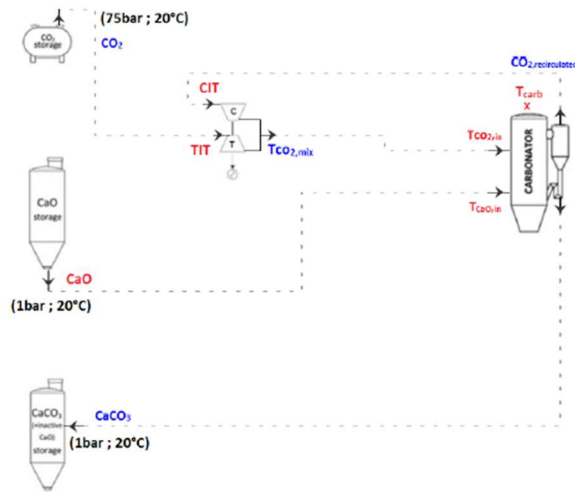
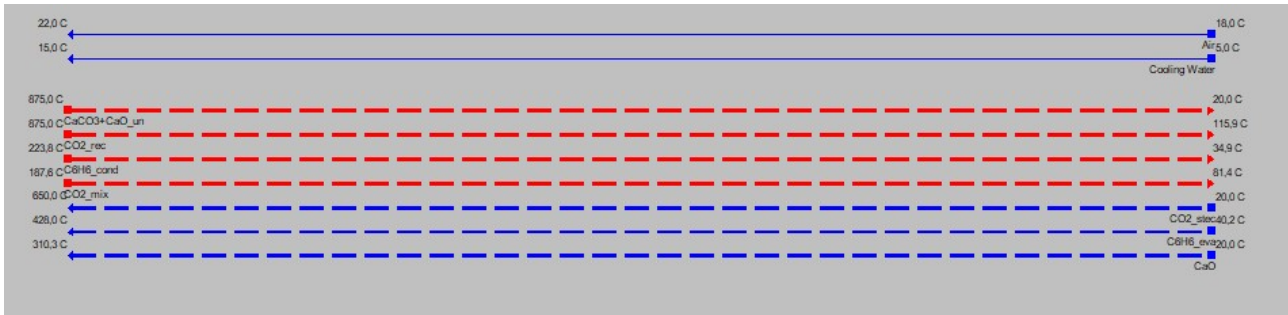
In the last two tables, selected values are the starting point of our analysis. Now, having explained how results have been obtained, we can proceed with the design of the heat exchange network.

4.2 A first design of the heat exchange network

The starting points of our analysis are the temperatures involved in the heat exchange and the values for the specific heat capacity within these intervals; the former are the ones reported in the previous tables, the latter are supplied by Tesio who obtained them for its thesis. In particular, the last ones are evaluated in specific intervals that come from the code used in MATLAB for the calculation of T* (the modified temperature used for the pinch analysis).

Now we can exploit all these data to design a first scheme for the heat exchanger network; in order to do this, a specific tool in the environment of Aspen is used, called Energy Analyzer. This is

necessary because fluids involved have specific heat capacities that are variable with the temperature, and this tool allows to insert all the segments of validity for each c_p . After the data import and the setting of the minimum temperature difference at 15°C, the situation is the one represented in the figure below.



Fluids involved	Tin (°C)	Tout (°C)	G (kg/s)
CaCO ₃ +CaO _{un}	875	20	2,697
CO ₂ _rec	875	115,9	1,372
C ₆ H ₆ _cond	223,8	34,9	3,724
CO ₂ _mix	187,6	81,4	2,132
CO ₂ _stec	20	650	0,761
C ₆ H ₆ _eva	40,2	428	3,724
CaO	20	310,3	1,936
Air	18	22	-
Cooling water	5	15	-

Figure 28 - Streams involved in the heat recovery network design (second scheme is reported from [2])

The fluids involved are the solid outlet stream exiting the carbonator (CaCO₃+CaO_{un}), the carbon dioxide recirculated from same outlet (CO_{2,rec}) the benzene streams respectively in condenser and evaporator (C₆H_{6,cond} and C₆H_{6,eva}), CO₂ streams respectively exiting the storage and entering the carbonator (CO_{2,stec} and CO_{2,mix}) and the solid stream of calcium oxide entering the carbonator (CaO).

With respect to the temperatures reported in previous tables, there is a little difference: the minimum temperature for the benzene is set to 34,9°C and not to 35°C; this choice has been made to solve a problem given by the tool, which didn't recognize the pinch points. In fact, in this scenario two pinch points are present (at 187,6/172,6°C and at 35/20°C respectively), but because of the approximation linked to the optimization algorithm (it's not the exact solution, but it converges to it with a very little tolerance), the grand composite curve at these pinch temperatures shows a value of the thermal flux very small and negligible with respect to other powers involved, nevertheless not exactly equal to zero. However, by changing the validity interval of the last c_p and thus changing

the extreme temperature from 35 to 34,9°C (and in practice with a negligible difference about thermal flux exchanged between fluids), the software succeeds in recognizing the two pinch points.

Moreover, two cold utilities have been inserted since the tool needs them in order to satisfy the cooling requirement; however, as we will see later, one of the cooling is referred to a solid stream and, since we have already said that solid outlets can be sent to storages at higher temperatures, we can avoid to take it into account.

Energy Analyzer gives us all the information about the pinch analysis, e.g. the composite curves and the grand composite curve, that are reported below.

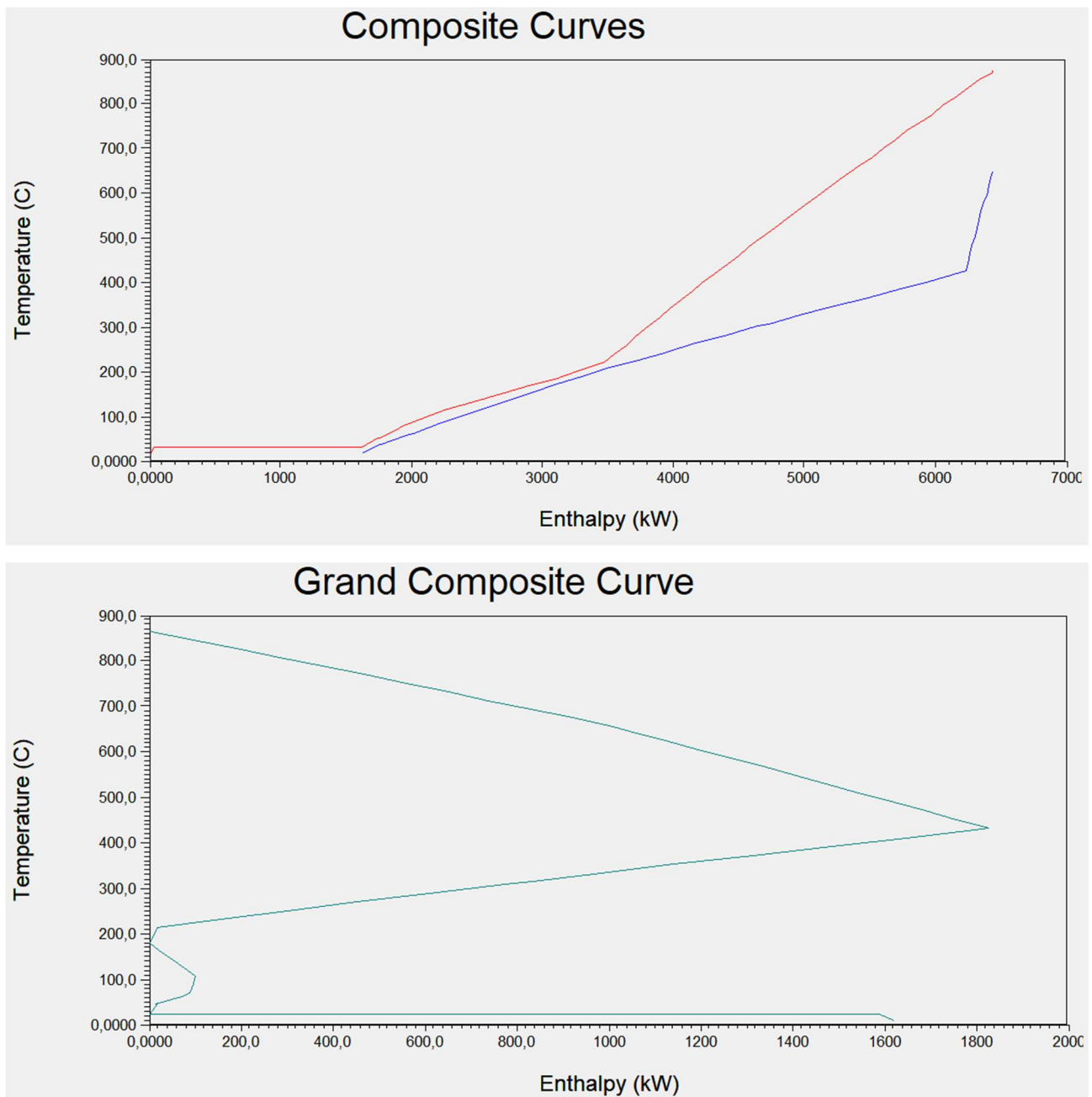


Figure 29 - Composite and grand composite curves

From the former of these graphs, we can notice the external heating requirement equal to zero and the cooling one involving the lowest temperatures (from software we know that it is equal to 1623 kW), whereas from the latter the two pinch points are more evident (at $T^*=180,1^\circ\text{C}$ and at $T^*=27,5$).

In order to understand the methodology involved in the design, we have to clarify some important points:

- initially, matches between solid streams have been avoided, since technology for heat exchange between solids isn't well developed, as already said and as suggested in literature [12]. However, as we will see later, this intention hasn't been maintained because of difficulties arisen during the design;
- splitting of the solid streams hasn't been initially considered, because it's more difficult than other splits involved [12], but also this purpose hasn't been fulfilled;
- as a general way to proceed, at each step of the coupling, fluids with the highest thermal flux to be supplied/received have been matched, with suitable fractions of split according to their products $G \cdot c_p$ (heat capacity flowrate or CP): when possible, splits have been conceived in order to have the same product both for hot and cold fluid and thus the same temperature difference at the exchanger extremes; in some steps of this method, however, it has been preferred coupling the fluids with the highest CP values (also here with suitable split fractions), in order to solve problems linked to their requirement satisfaction. This approach has been partially inspired by some studies with similar problems found in literature (e.g. Lara et al. [26], where the heat network design of a CaL system indirectly integrated with a supercritical steam cycle is analysed).

For simplicity, the design has been carried out by separating the fluids into two zones: above the 2nd pinch point (i.e. above $187,6^\circ\text{C}$ for hot fluids and $172,6^\circ\text{C}$ for cold ones) and below it.

Design here obtained are reported in the figure below.

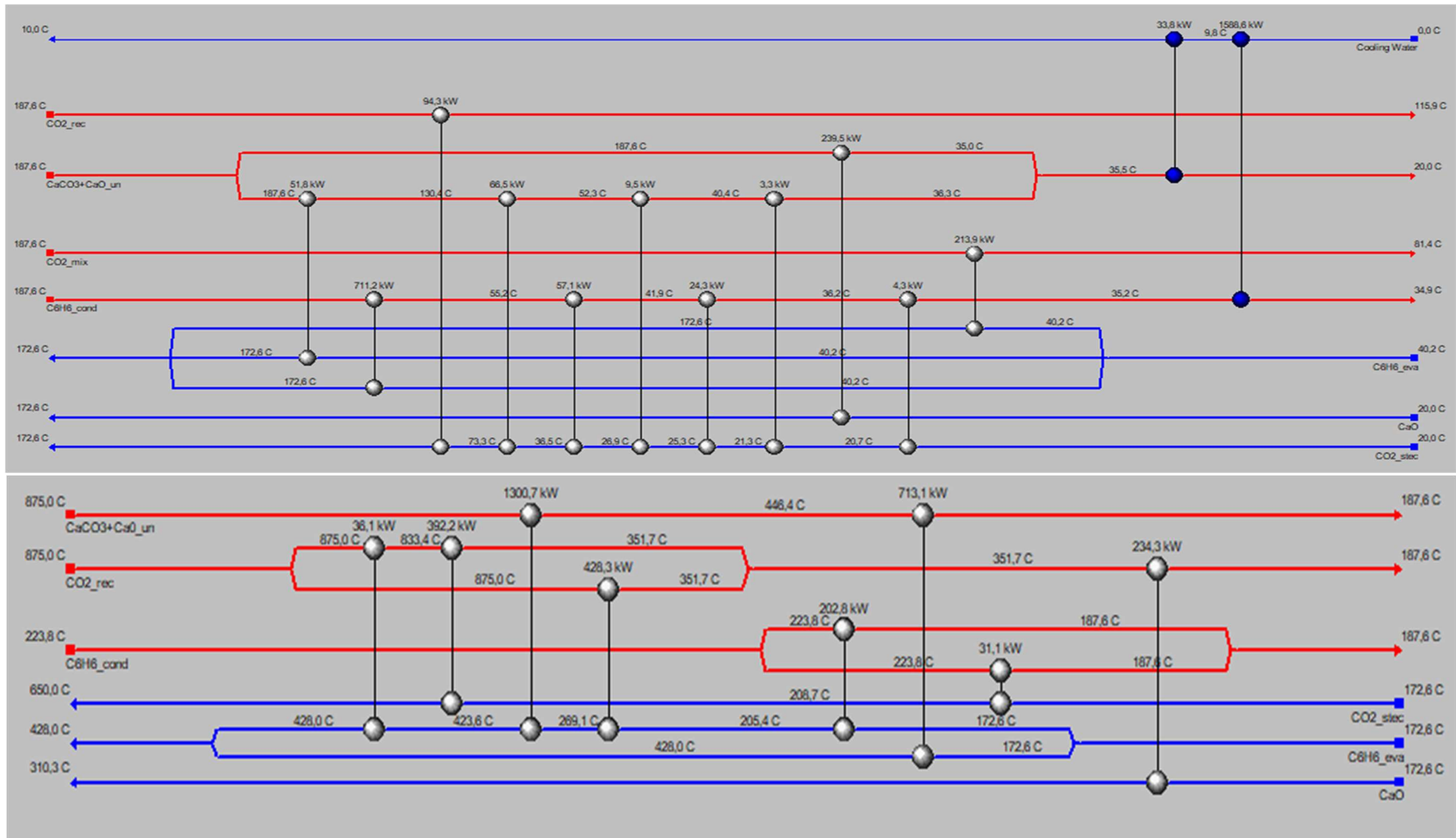


Figure 30 - Heat recovery network of the real plant respectively below and above the 2nd pinch point

FLUID	SPLIT FRACTIONS
CaCO ₃ +CaO _{un}	0,644
	0,356
C ₆ H _{6,eva}	0,728
	0,219
	0,053

Table 7-Fractions of split for fluids below the 2nd pinch point

FLUID	SPLIT FRACTIONS
CO _{2,rec}	0,5
	0,5
C ₆ H _{6,cond}	0,867
	0,133
C ₆ H _{6,eva}	0,734
	0,266

Table 6-Fractions of split for fluids above the 2nd pinch point

As we can see, in this configuration 20 heat exchangers are present (actually, there are 21 of them reported in the figure, but the cooler for CaCO₃ in practise is not considered, since, as already said, solid products streams can be sent into storages at higher temperatures with respect to the nominal ones), and, especially for the zone between the two pinch points, some of them are of little size, to avoid temperature difference problems. This difficulty in plotting the network is mainly linked to two aspects:

- the proximity of the two composite curves, that in the zone between the two pinch points maintain a distance a little higher than the pinch point one. Therefore, as already mentioned, in order not to have a temperature mismatch in a following coupling and thus to have the same temperature difference at the two extremes of a heat exchanger, in this zone each match has to be made between fluids with the same heat capacity flowrate CP (and so with parallel T-φ curves);
- specific heat capacities of the fluids involved are strongly dependent on temperatures (and thus CPs), and some of them represent also a problem for coupling.

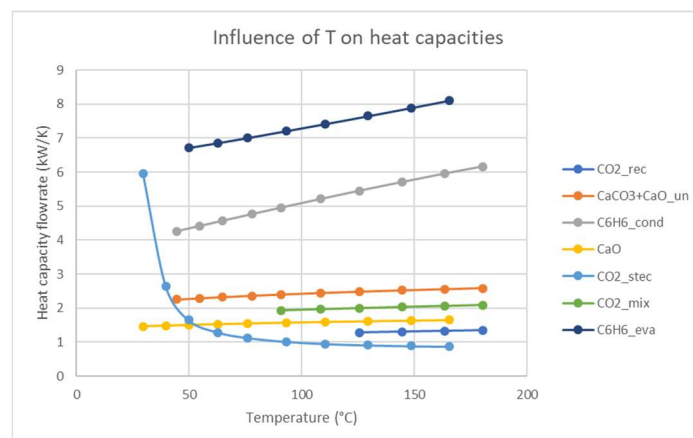


Figure 31 - Variation of heat capacity flowrates with the temperature

As we can observe from the graph above (where CP dependency on temperature in the zone between the two pinch points is reported), while most of the fluids' behaviours are almost linear with increasing T, the peak at low temperature for stoichiometric CO₂ represents a big problem for a correct coupling; moreover, also benzene presents a larger variation both in evaporation and condensation stages, but the similar slopes suggest us to try a coupling between the two fluids.

Analysing the network obtained in this step, we can certainly notice that the number of exchangers is high; this is a problem intrinsically related to the treatment of supercritical fluids, as already seen by Lara et al. [26] with supercritical steam cycle. In our case, however, the main problem is represented by heat capacities; therefore, to solve it, a possible option is to make some assumptions and simplifications about them, towards a sort of "linearization" that it will be explained in the next section.

4.3 Linearization of heat capacities and design simplification

The method exploited to simplify heat capacities is the following: except for the benzene in the condenser and the CO₂ exiting from storage (CO_{2,stecc}), all the c_p of the fluids have been subdivided into a number of them equal to the number of "zones" in which the fluid passes (i.e. two different heat capacities have been obtained for fluids which are present both in the zones above and below the 2nd pinch point, one c_p value for CO₂ entering the carbonator which is present only in the zone between the two pinch points and three c_p values for the others); for CO_{2,stecc} and C₆H_{6,cond}, instead, more subdivisions have been made, in order to face up to peaks and large increases in the real trends. Moreover, for C₆H_{6,cond} these further subdivisions are needed because, if we neglect them, external requirements for cooling and heating will increase (i.e. hot fluids composite curve will be different from real case and there will be uncovered portions of both the curves, that means thus a thermal requirements increase).

Each "equivalent" heat capacity has been obtained with a weighted average: since data obtained from Tesio regarding c_p were under the form of many intervals of temperature and their correspondent heat capacity for that fluid, the new value has been evaluated by multiplying each value of c_p times the temperature interval of validity, by summing all the results and by dividing the

value here obtained by the interval of temperature ΔT in which we have chosen to have the linearization. For a generic fluid j , the formula utilised is reported below:

$$c_{p,eq,j} = \frac{\sum_i^n c_{p,i,j} \cdot \Delta T_i}{\Delta T} \quad (10)$$

where n represents the total number of sub-intervals of validity ΔT_i for the single $c_{p,i}$.

The design obtained is reported in the next page (with a subdivision respectively in the upper region and in the zone between the two pinch points, whereas the lower region has not been represented since it's constituted of coolers which are the "extension" of the ones reported in the second scheme).

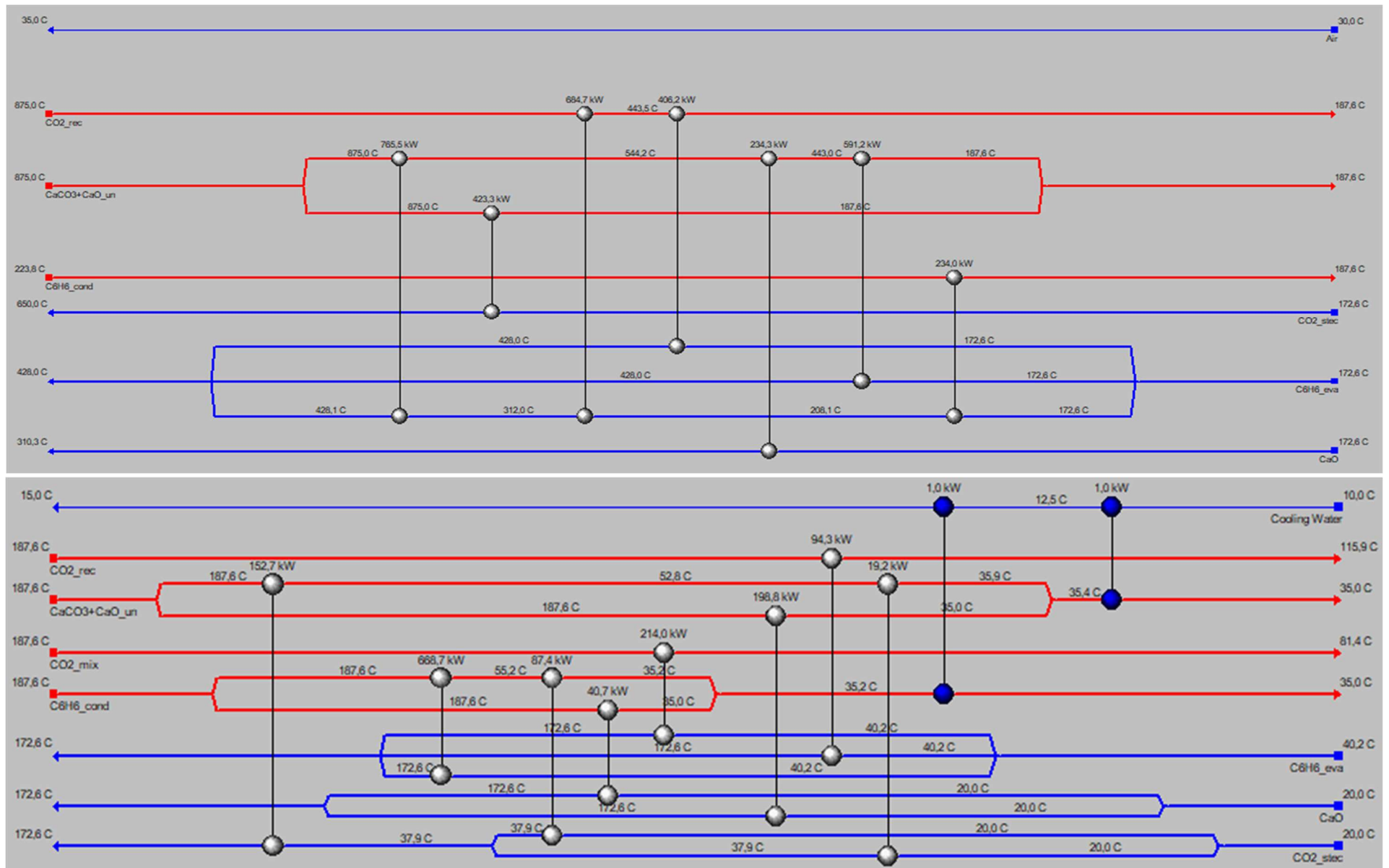


Figure 32 - Scheme of the zone above the 2nd pinch point and the middle region respectively

FLUID	FRACTION OF SPLIT
CaCO ₃ +CaO _{un}	0,790
	0,210
C ₆ H ₆ ,eva	0,628
	0,151
	0,221

FLUID	FRACTION OF SPLIT
CaCO ₃ +CaO _{un}	0,465
	0,535
C ₆ H ₆ ,cond	0,949
	0,051
C ₆ H ₆ ,eva	0,219
	0,685
CaO	0,170
	0,830
CO ₂ ,stec	0,180
	0,820

Table 8 - Fractions of split for fluids respectively in the upper and middle zone

The improvement is clear, since the design here obtained is composed of 16 effective heat exchangers (the cooler on calcium carbonate is obviously inexistent in practice, as previously explained).

To further improve the design, also Energy Analyzer itself has been exploited, with its function “Recommended Designs”: by inserting as input data the forbidden matches (here for simplicity all the couplings have been allowed), the maximum number of designs obtained and the maximum number of splits allowed for each fluid, the tool tries to find different “near-optimum” solutions for the design. The results, however, isn’t acceptable: in fact, the program seems to find only an economic optimum, without considering thermodynamic aspects and even violating the minimum temperature difference constraint (sometimes giving a negative difference between hot and cold side), losing any validity for our study. An example for the upper region is reported below, where the yellow heat exchanger is infeasible because $T_{hot}-T_{cold}$ assumes negative values.

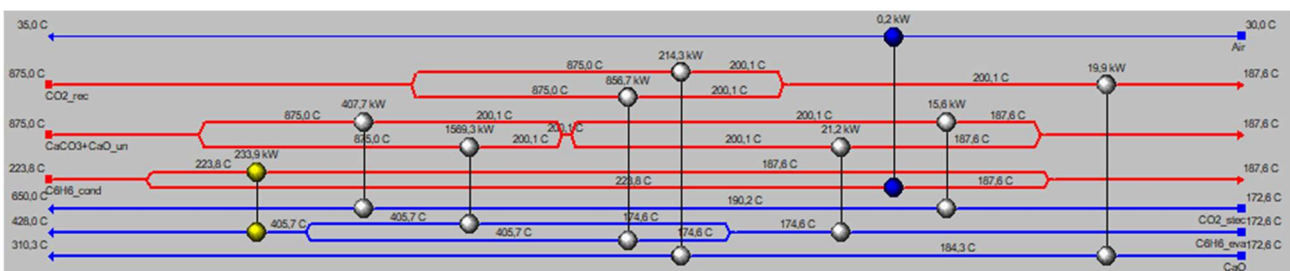


Figure 33 - Infeasible near-optimum plant designed by Energy Analyzer

In next chapters, our purpose will be to find the best feasible option from an economic point of view: by simplifying the heat exchange network with a specific methodology (that we will explain later), and assessing the cost for each new configuration, we will arrive to an optimum design, which of course will have higher external requirements, but a lower cost with respect to the already obtained scheme.

5 Economic improvement of the heat network

The methodology involved in the economic improvement of the plant is constituted of two main procedures:

- the simplification of the heat exchangers network, in turn constituted by the removal of the exchanger itself and the path of intervention in order to restore the minimum temperature difference;
- the economic evaluation of the obtained designs, in order to move towards an optimal situation.

Now let's see the main steps of these procedures.

5.1 Simplification of the heat exchangers network

The concept of simplification starts from the theory of graphs, utilised in general to describe systems with a complex topology: in fact, concepts like branches (i.e. oriented segments), nodes (i.e. points which limit branches) and meshes (i.e. closed independent loops constituted of branches) can be easily applied to the topology of heat recovery network. In particular, we can use the Euler's formula for planar graph [27]:

$$u = N + M - S \quad (11)$$

where

- u represents the number of branches, which, in our case, it is equal to the number of heat exchangers involved;
- N is the number of nodes. For heat recovery network, it is the number of internal fluids plus external sources;
- M represents the number of meshes (to be an independent mesh, a closed loop has to have at least one heat exchanger that other loops haven't);
- S is the number of subsystems, i.e. parts of the network that are totally independent one from each other (one subsystem is constituted of branches and nodes that are not in common with other subsystems).

Our purpose, from a pure economic point of view, is to reduce the number of heat exchangers, since, as we'll see in next chapters, this reduction means a direct reduction of investment costs for the plant. By observing the Euler's formula, it can be noticed that this kind of simplification can be carried out in two ways [27]:

- decrease of the number of meshes M ;
- increase of the number of subsystems S .

The latter solution is difficult to be exploited, since we have to distinguish two energetically balanced and separated networks, and that is a rare possibility for normal cases, in particular for ones with a complex network as in our case.

Our possible way to proceed can thus be the former one; of course, this is possible if $M > 1$, but at the same time its reduction leads to a very probable increase in the external requirements. By applying the Euler's formula to the real plant to calculate the number of meshes (considering also the cooler for the solid particles that in reality it's not considered), we obtain the following result:

$$M = u - N + S = 21 - 8 + 1 = 14 \quad (12)$$

Therefore, it can be possible to simplify this situation by lowering this number. Of course, by analysing the plant with equivalent specific heats, the improvement is clear:

$$M = u - N + S = 17 - 8 + 1 = 10 \quad (13)$$

Although the number of meshes is decreased, there is room for further improvements.

The main steps of the procedure exploited for this work is as follows:

- 1) selection and removal of the heat exchanger with the lowest power, but still belonging to a mesh. This last clarification is fundamental: in fact, in some steps of the simplification, the heat exchanger with the lowest thermal power doesn't belong to any mesh and, in step 2), it represents a problem for the re-assessment of the powers of heat exchangers left; moreover, the choice of the lowest power is due to the fact that, at most, the increase in external requirements will be equal to this value (but we will expect an even lower value). As an example, referred to the first simplification from the equivalent base case, one of the heat exchangers between $\text{CaCO}_3 + \text{CaO}_{\text{un}}$ and $\text{CO}_{2,\text{stec}}$ is chosen, with a flux $\phi = 19,18$ kW;
- 2) re-assessment of the thermal powers and temperatures involved in a mesh that previously contained the removed exchanger. In order to understand this step, it could be useful to

refer to the following scheme (in this example, is reported the scheme which explains the first simplification):

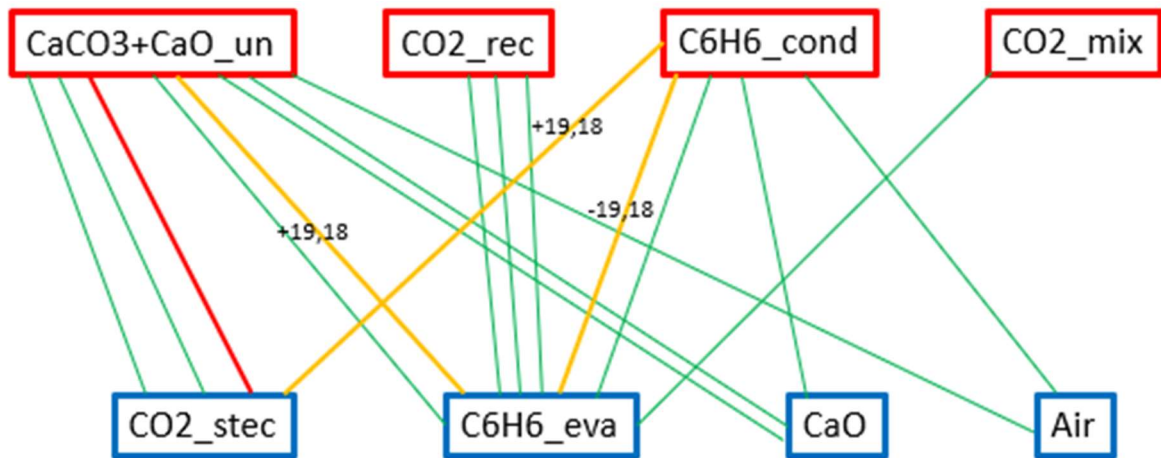


Figure 34 - Scheme used for the first simplification (in red, the removed exchanger, in yellow the other ones involved in the considered mesh, each one with its thermal power increase/decrease)

3) after the previous step, it can be possible to have one or more temperature differences that are smaller than the pinch point one, or even a mismatch temperature difference (one or even both the differences of a heat exchanger are negative, i.e. the hot fluid temperature has a lower value than the cold one); to establish again the minimum temperature difference, the way to proceed is to select what is called the “intervention path”. It is a path along the network that passes through at least one of the temperatures involved in the difference problem; moreover, it has to belong to one of the following subcategories:

- a) a closed path (i.e. another mesh). In our simplification, this type of path is not considered (only in the last simplifications, the re-assessment in step 2 will give a result similar to this type of path), since the consequent redistribution is quite complex and, in most of our cases, it doesn't solve totally the problem. Moreover, particularly for first steps, redistribution within a mesh would only move the problem of violation of minimum temperature difference to another point between the exchangers of the selected closed loop;
- b) an open path which starts in correspondence of an external source and ends in correspondence of another one. It is the type of path that we have used mostly in this work;
- c) an open path which starts in a point of entry of a hot fluid and ends in a point of exit of a cold one. Although apparently this solution could look useless (since it implies the addition of a heater/cooler, in contrast with the purpose of reducing the number

of exchangers), in some cases it is necessary because other types of path lead to an increase in external requirements that is higher than the flux of the exchanger removed.

- 4) After the selection of the path, we can proceed in a similar way with respect to step 2: there is a redistribution of a certain amount of flux between the heat exchangers being passed through by the path, in order to re-establish the pinch point difference. They can be involved in the path in two ways:

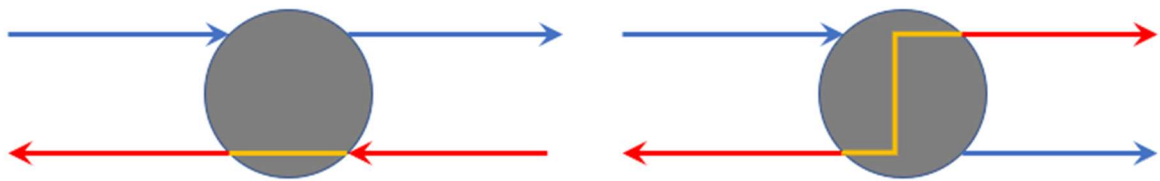


Figure 35 - Types of exchanger crossing by intervention path (in red they are represented the fluids involved in the path and in yellow the crossing of the exchanger)

In the first case, the path crosses the heat exchanger along a single side (hot or cold), so both the temperatures of it will change of the same quantity, leaving the flux unchanged; in the second case, the path crosses both the sides, thus changing the thermal power involved, which is redistributed between other exchangers crossed in a similar way (if there are) or between heaters and coolers (if involved in the path).

At the end of the intervention, in all the cases (except for the case a) within a mesh), the pinch point has moved from the original point; since this means that a heat exchanger has crossed the pinch point with respect to the original case, the minimum external requirements are increased.

Now we can fully understand and analyse the simplification of the plant carried out in this work. Starting from the base case, the first simplification clearly requires the addition of a heater for benzene passing through the evaporator ($C_6H_6_{eva}$), since in our original scenario no heating source was needed and thus no heating stage was present.

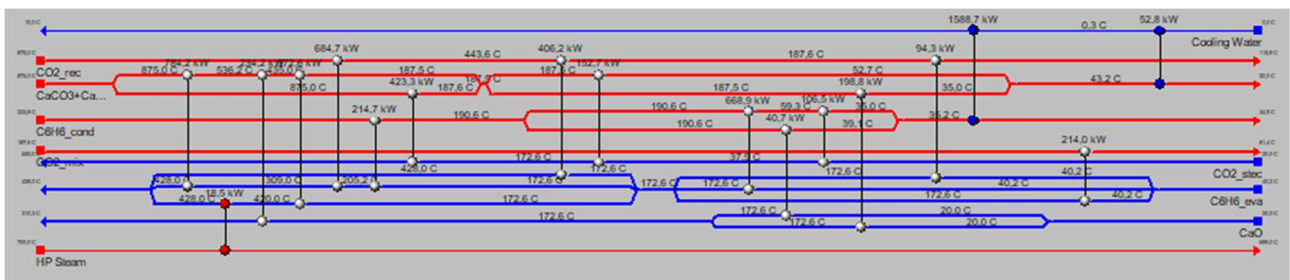


Figure 36 - Network after the 1st simplification

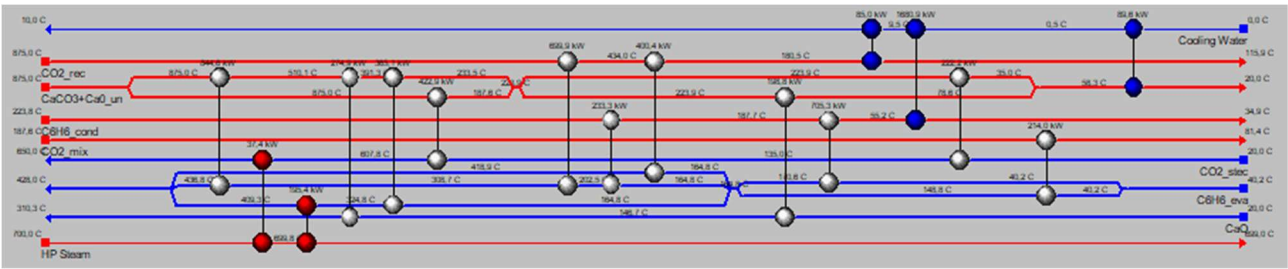


Figure 38 - Networks for Scenario 1 and 2 after the 4th simplification

For the fifth removal, things proceed normally, with a simplification in both the scenarios (for Scenario 1 there is neither an increase in the demands).

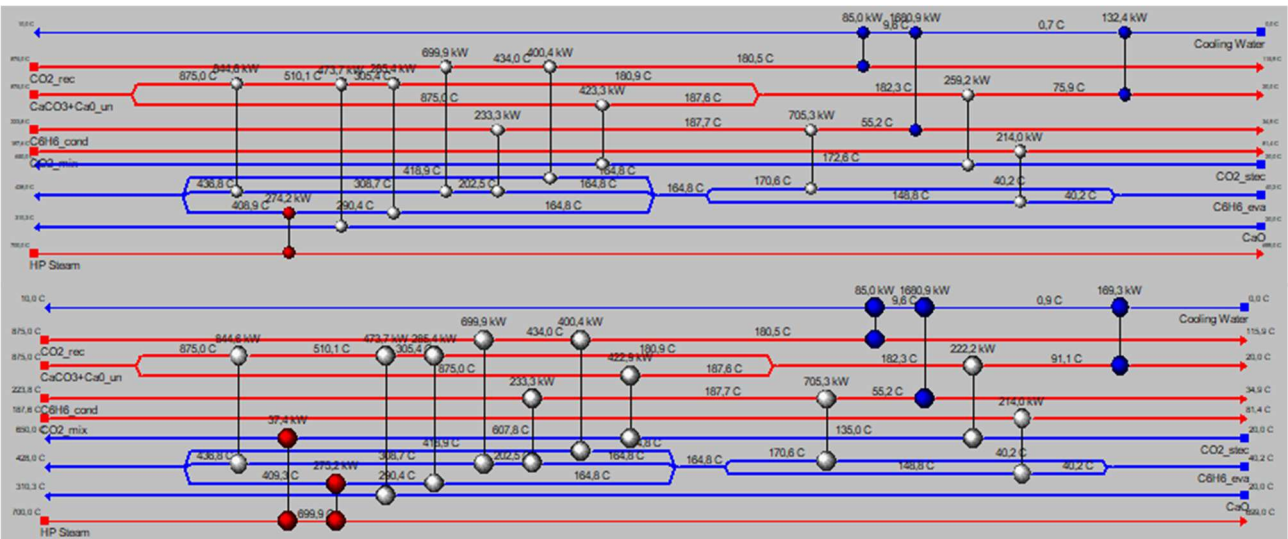


Figure 39 - Networks for Scenario 1 and 2 after the 5th simplification

For Scenario 1, in the 6th simplification, we could again have two way to go on, i.e. increasing only the requirements or adding a heater; we will refer to this subdivision as Scenario 1a and 1b, respectively.

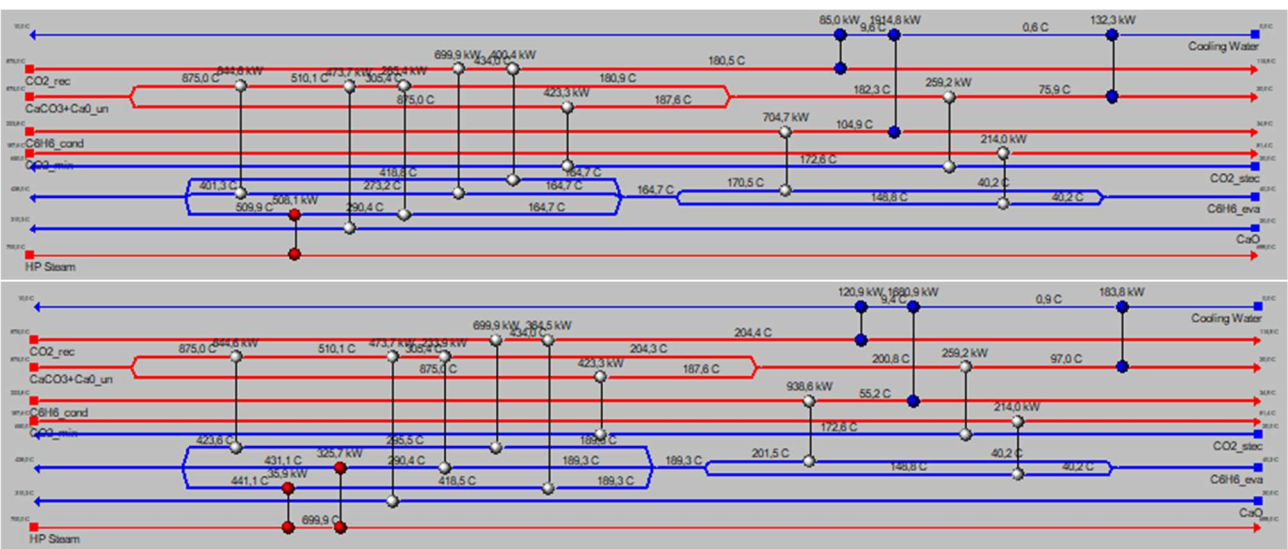


Figure 40 - Networks for Scenario 1a and 1b after the 6th simplification

For Scenario 2, instead, intervention is quite easy, since we only act on the external demands; however, as we will see from economic analysis (explained in next chapter but carried out in parallel with simplifications during the work), the trend is a strong increase of costs for this scenario, so further improvements from this step won't be considered.

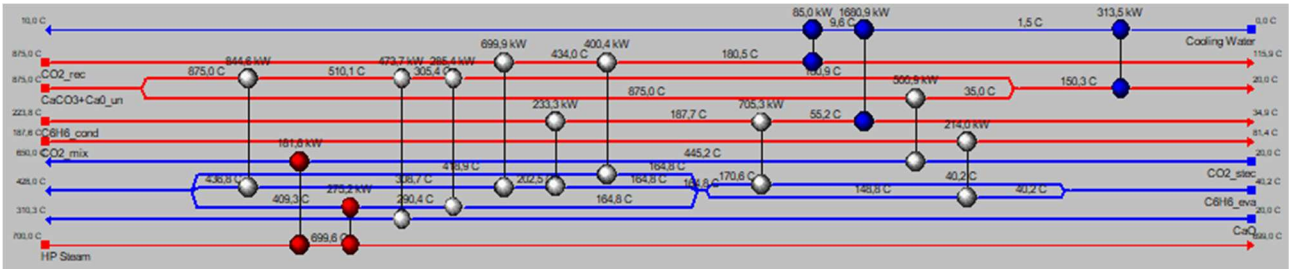


Figure 41 - Network for Scenario 2 after the 6th simplification

For the 7th simplification, in Scenario 1a the only feasible option is to add a heater, whereas an intervention on requirements is not possible: in fact, if we remove the selected exchanger and we try to redistribute the fluxes, we'll reach the infeasibility from a point of view of temperatures.

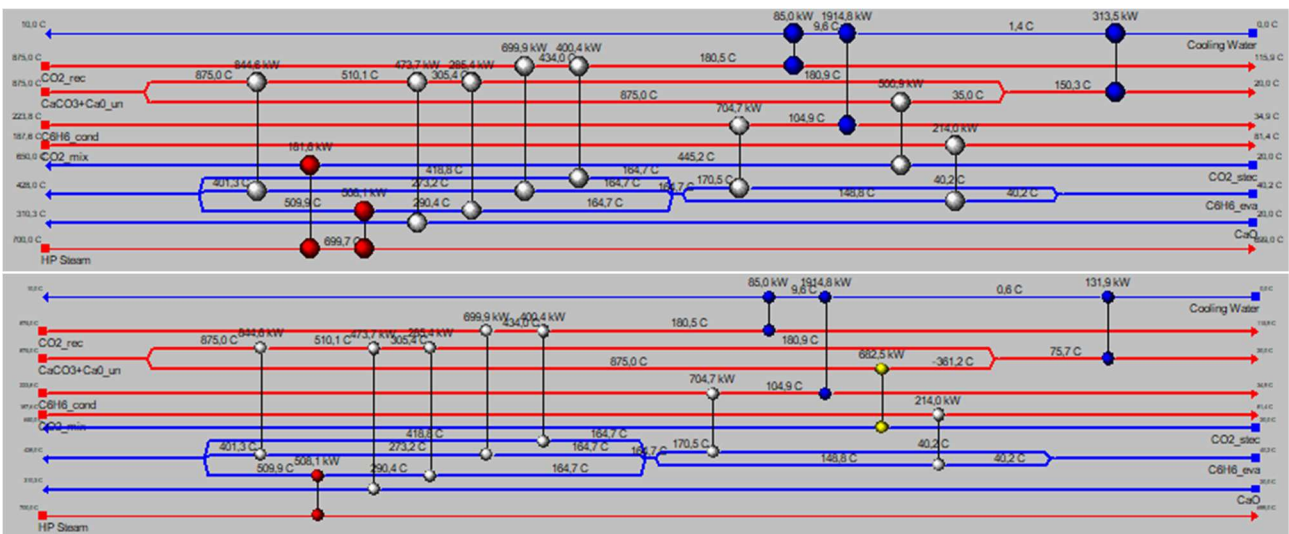


Figure 42 - Networks for Scenario 1a after 7th simplification with addition of a heater and with intervention on requirements (the second one is infeasible)

In Scenario 1b, instead, we can use the re-assessment/intervention within another mesh, so neither external requirements nor the number of exchangers will increase.

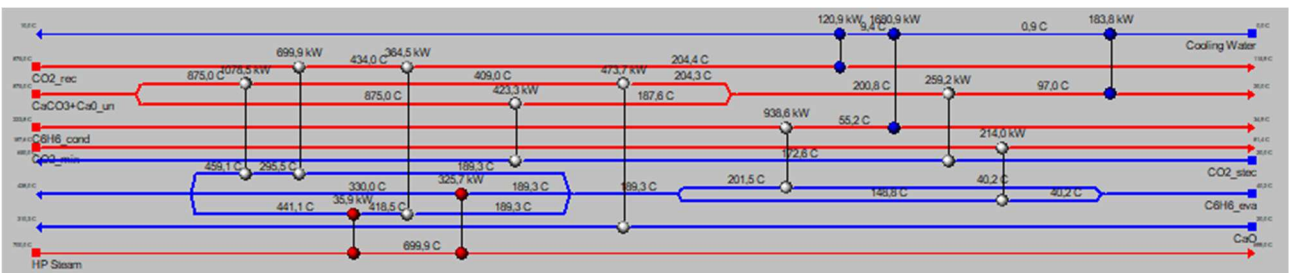


Figure 43 - Network for Scenario 1b after the 7th simplification

Last simplifications, which are carried out in Scenario 1b, slightly differ from previous ones: in fact, since for 8th simplification we would have to add again a heater (since other methods are infeasible), we have also tried to simplify the most expensive heat exchanger and not the one with the smallest flux, in order to reach a better situation from an economic point of view. For the “new” 8th simplification the purpose is reached, but for further one we do not succeed in doing it, so we do not continue the simplification work.

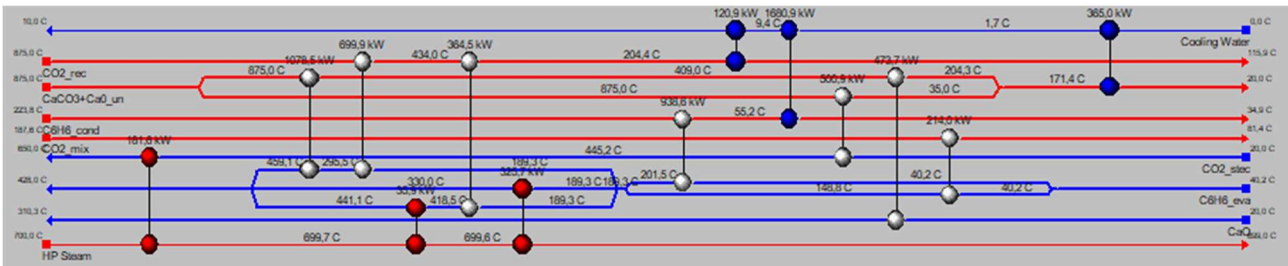


Figure 44 - Network for Scenario 1b after the 8th simplification adding a heater

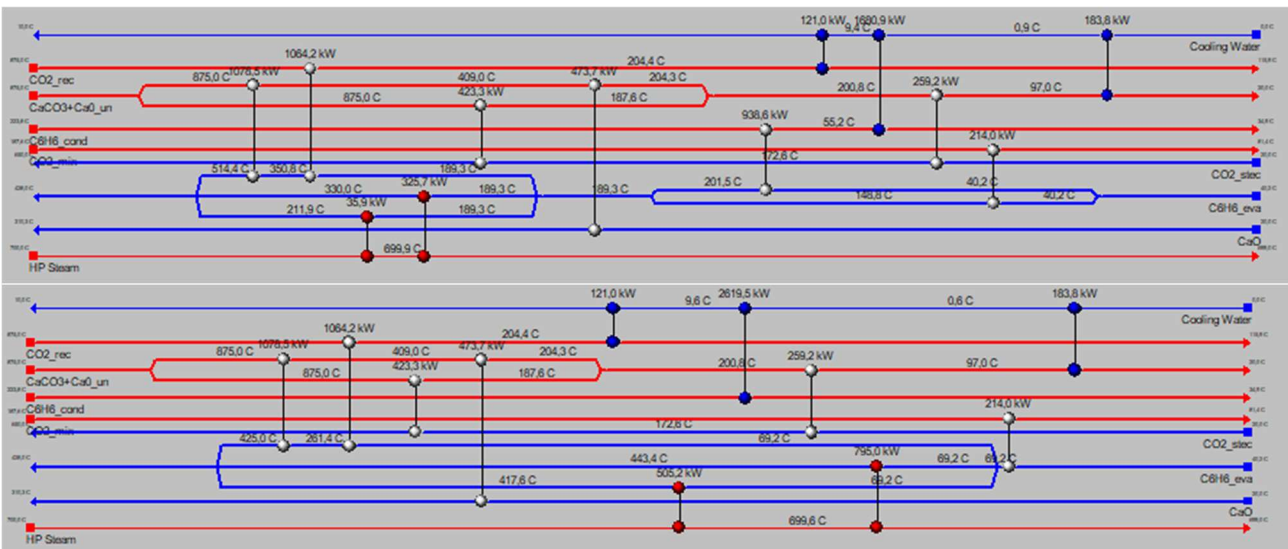


Figure 45 - Networks for Scenario 1b after 8th and 9th simplification by removing the most expensive exchanger

Here are summarized the results obtained.

Simplification	Flux removed in Scenario 1a (kW)	Change in external requirements (kW)	# of heat exchangers for 1a
1	19200	18520	17
2	40700	22040	16
3	94300	78940	16
4	106500	154700	15
5	198800	0	14
6	233300	233900	13
7	259200	181600	13

Simplification	Flux removed in Scenario 2 (kW)	Change in external requirements (kW)	# of heat exchangers for 2
1	19200	18520	17
2	40700	22040	16
3	94300	78940	16
4	106500	113300	16
5	198800	79800	15
6	222200	144200	14

Simplification	Flux removed in Scenario 1b (kW)	Change in external requirements (kW)	# of heat exchangers for 1b
1	19200	18520	17
2	40700	22040	16
3	94300	78940	16
4	106500	154700	15
5	198800	0	14
6	233300	87500	14
7	233900	0	13
8	364500	0	12
9	938600	938400	11

Table 9 - Resume of the simplifications achieved

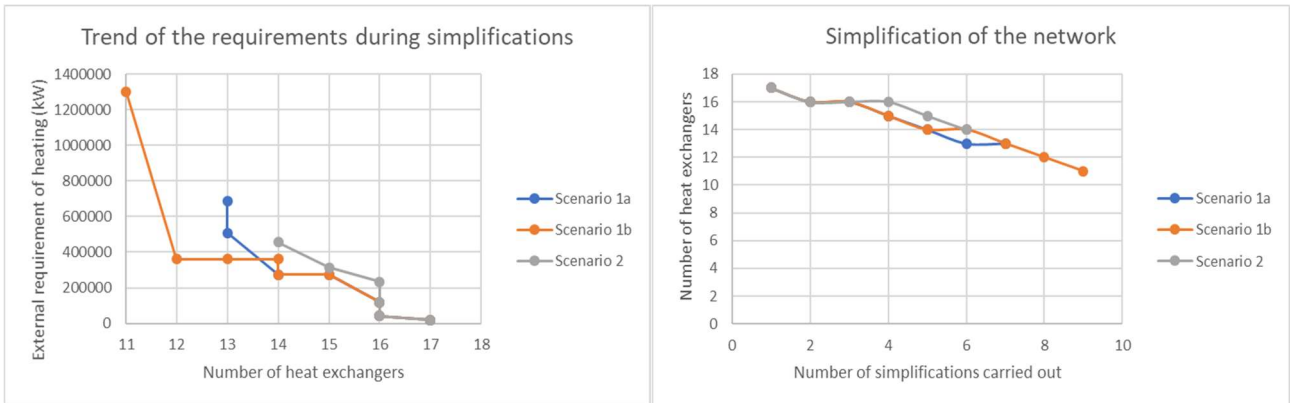


Figure 46 - Number of exchangers in the different scenarios and trend of the requirement

As we can see from tables above (and as previously said), some removals have not required a change in external needs: this is due to the fact that the re-assessment has taken place within a mesh composed of only two exchangers and, when we have removed the chosen one, the other one had a Logarithmic Mean Temperature Difference (LMTD) so high that the redistribution didn't create any temperature violations; this is a sort of case a) between intervention paths applied to redistribution. Moreover, we could not apply this kind of re-assessment (and also the related intervention path) in first simplifications because meshes under investigations in those steps were near one of the pinch points, so our intervention would have caused a temperature violation (with consequent requirement increase, thus losing any advantage with respect to our method).

Now, in order to fully analyse the work already done until now, we can introduce the method for the economic evaluation utilised here; as already mentioned, this type of analysis has been made in parallel with the simplification, in order to understand in which direction we were moving to.

5.2 Economic analysis of the obtained networks

Economic analysis employed in this work is based on guidelines and methodologies elaborated by the National Energy Technology Laboratory (NETL) of the U.S. Department of Energy (DOE) for the

cost estimation of power plants and systems [28]. This methodology has been developed by NETL in order to evaluate costs associated to a power plant and its components and to find out which configuration is the best from a pure economic point of view. Most techno-economic studies completed by NETL feature cost estimates intended for the purpose of a “Feasibility Study” (AACE Class 4, a classification for the Association for the Advancement of Cost Engineering) and this work doesn’t make an exception; for this class of study, the following features are expected, with a relevant error of the cost estimation with respect to the real value:

Project Definition	Typical Engineering Completed	Expected Accuracy
1 to 15%	<ul style="list-style-type: none"> • plant capacity, block schematics, indicated layout, process flow diagrams for main process • systems, and preliminary engineered process and utility • equipment lists 	-15% to -30% on the low side, and +20% to +50% on the high side

Table 10 - Features of an AACE Class 4 Cost Estimate [28]

Therefore, we have to pay attention to this high error with respect to the real value, but, since in this work we compare one scenario with each other, the error is the same for each scenario, fact that guarantees to obtain the best configuration although the unavoidable inaccuracies. Moreover, since each scenario differs from the others only for the heat exchanger network layout (and not for other components of the plant), our economic analysis is pointed only on it.

This methodology starts from capital cost of the components, i.e. the initial investment cost linked to them; in particular, the capital cost is defined at five levels, each of which takes into account a different information about the component:

- 1) Bare Erected Cost (BEC) takes into account the cost of process equipment, on-site facilities and infrastructure that support the plant and the direct/indirect work required for its construction and/or installation;
- 2) Engineering, Procurement and Construction Cost (EPCC) considers BEC plus the cost of services provided by the Engineering Procurement and Construction (EPC) contractor. It is usually an external service, since big companies pay some external societies in order to design, procure and construct their plant (while feasibility studies are usually done by big companies);
- 3) Total Plant Cost (TPC) includes EPCC plus process and project contingencies;

- 4) Total Overnight Cost (TOC) takes into account TPC plus all other “overnight” costs (=costs as we’re building the plant in one night, thus not considering the effect of time on capital cost due to inflation), including owner’s costs;
- 5) Total As-Spent Capital (TASC) includes TOC plus the effects of escalation and inflation and the interest during the construction.

Here are summarized the different levels.

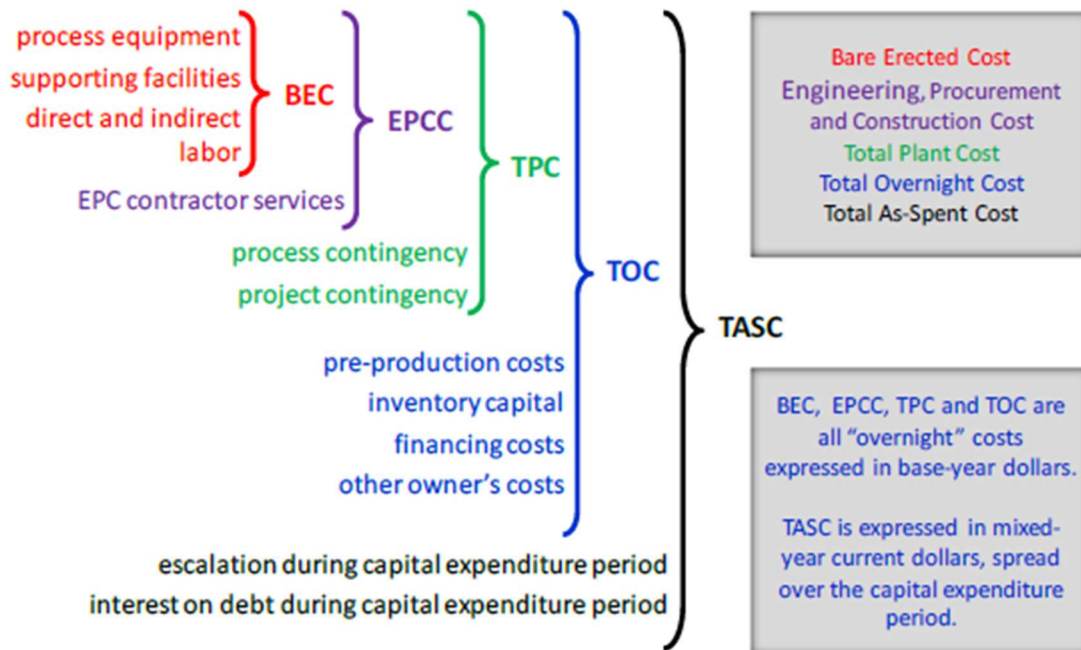


Figure 47 - Levels of the capital cost according to NETL [28]

Therefore, the starting point of our analysis is the estimation of the BEC of the heat exchanger network for each design.

5.2.1 Estimation of the BEC

According to NETL, the approach to estimate the BEC of a component involved in a power plant is based on cost functions, i.e. polynomial functions that have been derived from a very large database of capital costs of thermal components. They are given for a specific base condition and then reported to operating conditions thanks to multiplying factors: they depend on the specific equipment type, system pressure and materials of construction. As we are analysing only the heat exchanger network, we are interested in cost functions linked to these components.

There are two cost functions utilised in this work.

1) One cost function comes from [29] and has been used for gas-gas exchange, for cooling stage (air cooling), for heating stage (gas-gas exchange between flue gases from a combustion chamber and the stream to be heated) and for combustion chamber (taken into account for calculations); it has the following formula:

$$C_{BEC} = C_P^0 \cdot (B_1 + B_2 \cdot F_M \cdot F_P) \quad (14)$$

where:

- C_P^0 is the purchasing cost of equipment referred to base conditions (e.g. common material, ambient conditions);
- B_1 and B_2 are constants correlated from data in previous works and are dependent on the type of equipment;
- F_M is the material factor, which mainly depends on the operating temperature;
- F_P is the pressure factor, which depends on the operating pressure.

C_P^0 is given in the form:

$$\log_{10} C_P^0 = K_1 + K_2 \cdot \log_{10} A + K_3 \cdot (\log_{10} A)^2 \quad (15)$$

where:

- K_1 , K_2 and K_3 are constants which depend on the type of equipment involved;
- A is the size parameter and depends on the type of component too.

In this work, the following values have been used [29]:

type of exchange	model	A	K1	K2	K3	minimum A of validity	maximum A of validity
gas-gas, heating stage	shell and tube (U-tubes)	area, m2	4,184	-0,2503	0,1974	10	1000
cooling stage	air cooler	area, m2	4,0336	0,2341	0,0497	10	10000
combustion chamber	process vesse, horizontal	volume, m3	3,5565	0,3776	0,0905	0,1	628

Table 11 - Values for the evaluation of $C_{p,0}$

The value of A has been calculated differently according to the type of exchange:

- for gas-gas exchange, fluxes and Logarithmic Mean Temperature Differences (LMTDs) have been taken from Energy Analyzer, whereas the overall heat transfer coefficient U has been taken from literature, giving thus the value of the area from the formula

$$A = \frac{\Phi}{\Delta T_{m1} \cdot U} \quad (16)$$

- for heating stage, fluxes have been taken from Energy Analyzer, whereas U has been taken from literature. LMTDs have been evaluated according to the number of stages:

- if there is only one heating stage:

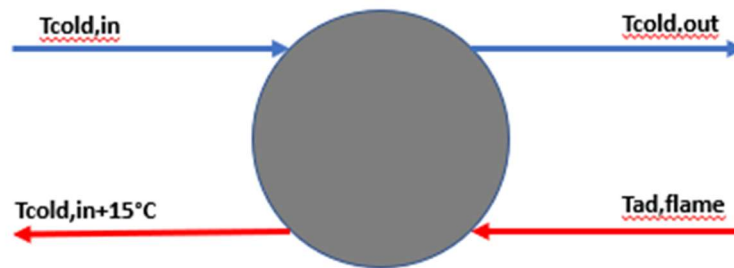


Figure 48 - Temperatures in case of a single heating stage

- if there are more heating stages, flue gases flowrate is evaluated according to the maximum heating request (we'll see in next sections) whereas temperatures are arranged in this way (here are reported the case with two heating stages, but similar considerations can be made for three):

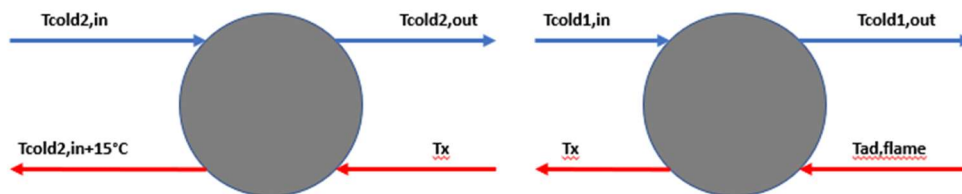


Figure 49 - Temperatures in case of multiple heating stages

where T_x is calculated with a trial-and-error in order to satisfy the requirements and the other constraints.

- For cooling stages, things are quite similar to heating stages, with small differences:
 - for single cooling stages, LMTD equal to 15°C;
 - for multiple cooling stages, for first cooling stage (the one with highest power) LMTD equal to 15°C, then it has been calculated the air flowrate passing through it in order to evaluate the temperature at the outlet of the second stage; from this, LMTD of the second stage has been evaluated.
- For the combustion chamber, volume has been evaluated by assessing the mean volume flowrate within it (as an arithmetic mean between inlet and outlet flowrates, as we will see) and then by multiplying it by a residence time of 0,5 s.

If the value of A is out of the acceptable range, it is scaled according to the six-tenths rule:

$$\frac{C_1}{C_2} = \left(\frac{S_1}{S_2}\right)^{0,6} \quad (17)$$

where:

- C_2 is the cost evaluated with the given equation with size parameter S_2 equal to the nearest limit value;
- S_1 is the size parameter of the real component.

Here are tabulated the value of U used in this work.

Type of exchange	U (W/m ² K)	Reference
C ₆ H _{6,eva} -gas	248	[30]
C ₆ H _{6,cond} -CO _{2,ste} c	90	[31]
CO _{2,rec} -CO _{2,ste} c	100	[32]
Air-gas	35	[33]

Table 12 - Values of U assumed

F_P can be evaluated in two ways:

- If operating pressure P (in barg = bar-1) is higher than ambient one:

$$\log_{10} F_P = C_1 + C_2 \cdot \log_{10} P + C_3 \cdot (\log_{10} P)^2 \quad (18)$$

where C_1 , C_2 and C_3 are constants coming from the regression process from real data.

Since we only have two types of component in pressure in our study (gas-gas exchanger and heating stage) that however have been modelled in the same way, this is the only possibility for parameters involved:

type of exchange	model	C_1	C_2	C_3	Min P	Max P
gas-gas, heating stage	shell and tube (U-tubes)	-0,00164	-0,00627	0,0123	5	140

Table 13 - Values to evaluate F_P

- If operating pressure is equal to 1 bar, F_P is unitary. This is the case of all the exchangers involving carbonator side streams and combustion chamber.

F_M in our work has assumed only three values:

- $F_M=2,75$ for heat exchangers with operating temperature above the 2nd pinch point, because in this case the use of stainless steel (SS) for both the shell and tube is advisable;
- $F_M=1$ for heat exchangers below the 2nd pinch point, because here we can use the carbon steel (CS);
- $F_M=7,1$ for combustion chamber, that operates at higher temperatures, so it needs a nickel (Ni) alloy as material.

It is advisable, while choosing the materials, to control whether they give problems about corrosion with benzene or not; this type of test has been carried out and it has been found that neither SS nor CS have any problem with C₆H₆ [34].

B₁ and B₂ depend on the type of equipment involved:

Equipment type	B1	B2
Gas-gas, heating stage	1,63	1,66
Air cooling	0,96	1,24
Combustion chamber	1,49	1,52

Table 14 - Values of B1 and B2 used

- 2) The other cost function has been obtained from the work of Albrecht et al. [35] on shell-and-plate exchangers between solid particles and supercritical CO₂ at high temperatures (550-750°C). It has the following form:

$$C_{BEC} = 18,4784 \cdot (UA)^{0,67} \cdot P^{0,28} \quad (19)$$

In our work, we have used this correlation both for solid-gas/liquid and solid-solid heat exchangers (since the latter, in our hypothesis, consist of two solid-gas heat exchangers where a suitable heat transfer medium transports the heat from a solid to the other one).

As a value for pressure (P) it can be assumed the maximum one between the two streams involved; for the product of the overall heat transfer coefficient times the heat transfer area (UA) we can easily obtain it from the flux and the LMTD from Energy Analyzer:

$$UA = \frac{\Phi}{\Delta T_{ml}} \quad (20)$$

For solid-gas/liquid exchange, ΔT_{ml} can be directly taken from value given by the software, whereas for indirect solid-solid heat exchange it can be easily demonstrated that, in case of a medium which transfers heat between two streams, LMTD of one of the two indirect heat exchangers is the half of LMTD that we would have in case of a single exchanger:

$$\Delta T_{ml,ind.exchanger} = \frac{1}{2} \cdot \Delta T_{ml,Energy Analyzer} \quad (21)$$

Moreover, the result obtained from this function is valid for high temperatures, because, as already said, the work from which it has been obtained is about an exchanger operating at them; in order to take into account lower temperatures (since there is no F_M in this formula), it has been assumed that, below the 2nd pinch point, the cost function is still valid with a sort of “correction factor” given by the proportion of F_M :

$$C_{BEC,low T} = \frac{1}{2,75} \cdot C_{BEC,high T} \quad (22)$$

Once we have all the BECs, before passing to next level of costs we have to consider the time the cost functions are referred to: in fact, these cost functions often refer the price of a component to

a specific year and, since time has an effect on costs (because of the different value of money, inflation and escalation), the price for a specific component in a specific year is different from the price of the same component for a different year. In our case, the first function is referred to 2001, while the second one to 2018; we can refer all the prices to 2018 by applying the following formula to the BECs obtained for 2001:

$$\frac{C_{BEC,2018}}{C_{BEC,2011}} = \frac{I_{2018}}{I_{2011}} \quad (23)$$

where I=cost index of a specific year; in particular, in this work it has been used values from Chemical Engineering Plant Cost Index (CEPCI), which are calculated using various data from the U.S. Bureau of Labor Statistics. Values utilised are reported in the table below.

Year	CEPCI
2001	397
2018	603,1

Table 15 - Values used for CEPCI [36]

5.2.2 Estimation of the EPCC

Concerning with EPCC level, there's an approach based on multiple subcontracts: as already said, engineering, procurement and construction are entrusted to external companies, but in multiple subcontracts to different subcompanies. This approach provides the owner with greater control of the project, while minimizing (or eliminating in some cases) most of the risk premiums that he has to pay to subcompanies: in fact, in a traditional lump-sum arrangement with only one EPC contract, the contractor assumes all the risks for performance, schedule and cost, so he asks for a premium in order to sustain it and, as a consequence, costs increase [28].

Following the guidelines of NETL, EPCCs in this work are estimated at 8% of the BEC, so they have been calculated starting from the BEC of each component obtained in the previous step.

5.2.3 Estimation of TPC

Concerning with TPC level, capital cost contingencies are very difficult to estimate, due to uncertainties that occur in constructing a thermal system (lack of complete project definition and engineering) [28].

Process contingencies depend on the specific process that we are considering: if this process is mature from a technological point of view, we can consider that these contingencies are almost zero. In the following figure, guidelines for their estimation are reported:

Technology Status	Process Contingency (% of Associated Process Capital)
New concept with limited data	40+
Concept with bench-scale data	30-70
Small pilot plant data	20-35
Full-sized modules have been operated	5-20
Process is used commercially	0-10

Table 16 - Process contingencies according to maturity [28]

For our case, SOCRATCES project is at a level of small pilot plant data; although we have to deal mainly with heat exchangers and combustion chambers (components that are widely spread and used commercially), the type of general process behind the CSP-CaL integration is in an experimental phase and even some types of exchangers are innovative. For these reasons, in this work process contingencies have been estimated at 30% of the EPCC.

Project contingencies, instead, for this work are estimated at 15% of EPCC + process contingencies.

5.2.4 Estimation of TOC

Concerning with TOC level, it represents all the costs that the owner has to face up to before starting the operations of the plant. These costs consist of [28]:

- prepaid royalties, that in our case are included in the associated equipment cost and thus not included as a cost to the owner;
- pre-production (start-up) costs, which include all the costs in order to do some preliminary tests and runs of the plant before starting. In our work, they're evaluated at 2% of TPC;
- working capital, for which no additional costs are included in our work;
- inventory capital, which is mainly related to fuel stocks and other consumables that have to be provided in order to allow preproduction activities. Since spare parts are the most

expensive contribution to this term, we can take their cost as a value for it, that is estimated at 0,5% of TPC;

- land, due to rent/purchase, but also its preparation for the plant installation. In general, it is estimated at 3000\$/acre, with an average occupation of 300 acres for IGCC and 100 acres for NGCC. However, in this work it has been chosen not to consider it: in fact, since our purpose is to compare scenarios all composed of heat exchangers and combustion chambers, which differ one from each other for a small number of them (and that doesn't represent a great difference from a point of view of land occupation), the land cost contribution has been neglected in all the scenarios, also because its value wouldn't have been so different from case to case;
- financing cost, which covers the cost of securing financing, including fees and closing costs but not including interest during construction. It has been estimated at 2,7% of TPC;
- other owner's costs, which include:
 - preliminary feasibility studies;
 - economic development;
 - construction and/or improvement of transport infrastructures near the plant;
 - legal fees;
 - permitting costs;
 - third-part evaluation of EPC contractor;
 - contingency (a sort of "management reserve").

They have been estimated at 15% of TPC.

For this work, TOC total contribution is evaluated at around 20,2% of TPC.

5.2.5 Estimation of TASC

In order to pass from overnight costs (TOC) to TASC, we need to estimate the interest during construction period. To do this, two types of financial structure are introduced:

- 1) in case of Investor-Owned Utility (IOU), the investor is also the figure (stakeholder) that invests more in the plant and owns it. This solution, suitable for smaller plants, permits to have a debt lower than (or at most equal to) 50% of the investment (i.e. the owner/investor

has to ask for a loan that is lower than the half of the total cost) and a relative lower interest (about 8,25-9,075%);

- 2) in case of Independent Power Producer (IPP), the ownership of the plant is independent of the institution that provided most of the capital. It is the most advisable solution for bigger plants, since the initial investment is higher, but consequently the debt is always higher than equity (between 60-70% of the total investment) and the interest that is applied is higher.

According to the financial structure, NETL suggests some corrective factors to obtain TASC from TOC by multiplication:

Finance Structure	High Risk IOU		Low Risk IOU	
Capital Expenditure Period	Three Years	Five Years	Three Years	Five Years
TASC/TOC	1.078	1.140	1.075	1.134
Finance Structure	High Risk IPP		Low Risk IPP	
Capital Expenditure Period	Three Years	Five Years	Three Years	Five Years
TASC/TOC	1.114	1.211	1.107	1.196

Table 17 - Multiplying factors to obtain TASC from TOC [28]

For the plant under investigation, it has been chosen an IOU scenario with a capital expenditure period of three years: in fact, in SOCRATCES project the owner is a consortium of companies, each of which produces and/or carries out R&Ds in the field of the project itself, so they provide also the capital in terms of provided components; moreover, each step of the project lasts on average three years, so we have assumed this period as the capital expenditure period. In addition, since preliminary studies of the project have fully analysed the entire process just in order to lower the risk associated to immature technologies, we have also assumed a Low Risk Scenario.

For all these reasons, the multiplying factor to pass from TOC to TASC is 1,075. For each design analysed, TASCs of all the components involved have been obtained from respective TOCs.

Now, in order to obtain our objective, i.e. the Levelized Cost Of Electricity (LCOE), we have to quantify the effect of time on the costs of component; in other words, we have to spread the costs over time but including the inflation and other effect of time on money. To do that, we firstly have to evaluate the Weighted Average Cost of Capital (WACC), which, since it is equal for all the scenarios, is evaluated one-off.

5.2.6 Estimation of WACC

To evaluate the effect of time on the investment capital, a suitable approach is the one based on the Discount Cash Flow (DSF) methods and, in particular, on the discount rate. It must be chosen considering:

- the real, risk-free discount rate referring to other possible investment as a basis;
- inflation during the whole lifetime of the project, that reflects the loss of purchasing power of the capital invested in the same period;
- a premium to be assigned to its own equity capital as a metric of the expected rate of return from a risky investment.

The discount rate that we will find will be thus equivalent to the cost of the capital, because it tells us which is the cost of investing a certain capital. It can be calculated using the Weighted Average Cost of Capital (WACC), that obviously has to take into account the financial structure of our investment:

$$WACC = K_E \cdot \frac{E}{E + D} + K_D \cdot \frac{D}{D + E} \quad (24)$$

where:

- E and D represent the percentage of equity and debt in our investment, respectively;
- K_E and K_D represent the costs of equity and debt, respectively.

E and D are given from the financial structure that we have chosen; in our case, an IOU Low Risk Scenario gives a structure of E=50% and D=50%.

K_E and K_D can be evaluated as follows:

- K_E accounts for two components:
 - a specific risk of the investment;
 - a systemic risk that depends on the evolution of the economy as a whole.

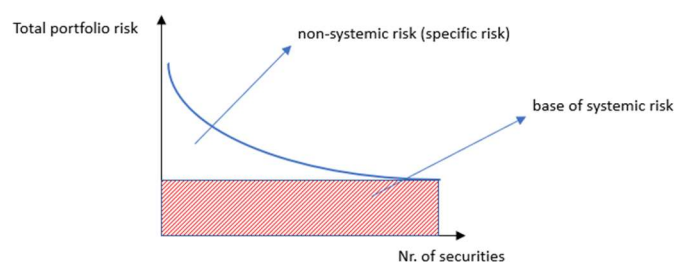


Figure 50 - Risk as a function of the number of investments

We are not in the situation of an investment composed of a high number of sub-investments, so the formula that define our K_E is the following:

$$K_E = R_f + \text{premium} \quad (25)$$

where:

- R_f is the systemic risk; it can be assumed as the government bond at short term, since it is the investment with the lowest risk. In our case, for simplicity it has been chosen the value of Italian BTP 10 years, therefore $R_f=1,046\%$ [37];
- the premium expected by the investor is given by the formula:

$$\text{premium} = R_S + \beta \cdot (R_m - R_f) = R_S + \beta \cdot EMRP \quad (26)$$

with:

- R_S is the small stock premium due to reduced liquidity and is only for small investors, so in our case $R_S=0$;
- $EMRP=R_m-R_f$ is the Equity Market Risk Premium (as a difference between the market return and the systemic risk) and represents the average interest that I can obtain investing in the market. In our case, $EMRP=5,5\%$ [38];
- β is a correction factor that is specific for the investment we are doing; in our case, we can assume $\beta=1$.

Therefore, we have obtained a premium of 5,5%.

As a consequence, K_E assumes a value of 6,546%.

- K_D has the following form:

$$K_D = IRS + \text{spread} \quad (27)$$

where:

- IRS is the Interest Rate Swap and represents the differential between a fixed and a variable interest, a sort of reference cost of the debt. In this study, $IRS=0,06\%$ [39];
- spread is the increase of the interest rate depending on the capability of the investor to return the capital; it has been assumed as the revenue for the bank, and thus $\text{spread}=1\%$.

For all these reasons, $K_D=1,06\%$.

By applying all the information explained before, we have obtained the following result:

$$i = WACC = 3,803\% \quad (28)$$

in the following table, results have been summarized.

Rf	1,046
Rs	0
EMRP=Rm-Rf	5,5
β	1
premium	5,5
Ke	6,546
IRS	0,06
spread	1
Kd	1,06
E	50
D	50
WACC	3,803

Table 18 - Data employed to obtain WACC (all data are in %)

Before proceeding to annuity calculation, it is useful to evaluate the fuel flowrate necessary in the designs where heating stages are present.

5.2.7 Calculation of the fuel flowrate and combustion chamber volume

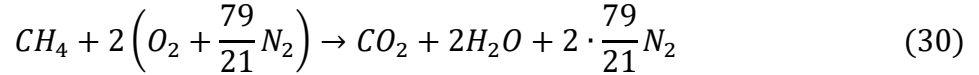
As previously anticipated, heating stages that are present in the designs are fed with the exhaust gases exiting from a combustion chamber, for our choice in turn fed with natural gas as fuel (being one of the less polluting fossil fuels). To assess the fuel flowrate needed to provide the requested amount of energy, the first step is to assume a temperature for flue gases exiting the chamber; in our case, we have chosen to assume the adiabatic flame temperature (T_{ad}) for natural gas (that, for simplicity, has been assumed as only formed by methane (CH_4)). Although in real combustion these temperatures are not achieved, we have taken into account the non-adiabaticity of the real reaction in other ways (we'll see in a while). For methane, T_{ad} is equal to 2236 K [40]; with this temperature can be evaluated the corresponding specific heat of exhausts: thanks to the utilization of a properties calculator [41], a c_p of 1364 J/kgK has been obtained.

Next step consists in finding the flue gases flowrate needed in order to satisfy the demand: as already introduced, in case of a single heating stage the flowrate is evaluated according to the only demand that is present, whereas in case of multiple heating stages is evaluated according to the highest demand but iteratively assessing an outlet temperature from 1st stage that allows to have all the other demands satisfied and a final temperature difference (at the outlet of the last heating

stage) of 15°C. After having chosen adequately the order of heating stages and respective temperatures, flue gases flowrate is thus evaluated as:

$$\dot{m}_{flue\ gases} = \frac{\Phi_{highest\ demand}}{c_{p,flue\ gases} \cdot (T_{ad} - T_x)} \quad (29)$$

In order to obtain any information about the fuel, we have to exploit the reaction of CH₄ combustion (we assume, for simplicity, the stoichiometric complete combustion of methane):



In fact, after having evaluated both the density in normal conditions and in real ones of the exhausts as follows:

$$\frac{kmol_{flue\ gases}}{kmol_{CH_4}} = 1 + 2 + 2 \cdot \frac{79}{21} = 10,52 \quad (31)$$

$$\rho_{N,flue\ gases} = \frac{MW_{CO_2} \cdot 1 + MW_{H_2O} \cdot 2 + MW_{N_2} \cdot 2 \cdot \frac{79}{21}}{10,52 \frac{kmol_{flue\ gases}}{kmol_{CH_4}} \cdot 22,4 \frac{Nm^3_{flue\ gases}}{kmol_{flue\ gases}}} = 1,23 \frac{kg_{flue\ gases}}{Nm^3_{flue\ gases}} \quad (32)$$

$$\rho_{flue\ gase} = \rho_{N,flue\ gases} \cdot \frac{293,15}{T_{ad}} = 0,162 \frac{kg_{flue\ gases}}{m^3_{flue\ gases}} \quad (33)$$

we can now evaluate the volumetric flowrate (both in real and normal conditions):

$$\dot{V}_{N,flue\ gases} = \frac{\dot{m}_{flue\ gases}}{\rho_{N,flue\ gases}} \quad (34)$$

$$\dot{V}_{flue\ gases} = \frac{\dot{m}_{flue\ gases}}{\rho_{flue\ gases}} \quad (35)$$

To pass from information about flue gases to one about methane (in stoichiometric quantity) is quite easy:

$$\dot{n}_{CH_4} = \frac{\dot{V}_{N,flue\ gases}}{22,4 \frac{Nm^3_{flue\ gases}}{kmol_{flue\ gases}} \cdot 10,52 \frac{kmol_{flue\ gases}}{kmol_{CH_4}}} \quad (36)$$

$$\dot{V}_{N,CH_4,stoic} = \dot{n}_{CH_4} \cdot 22,4 \frac{Nm^3_{CH_4}}{kmol_{CH_4}} \quad (37)$$

$$\dot{V}_{CH_4,stoich} = \dot{V}_{N,CH_4,stoich} \cdot \frac{T_{CH_4}}{T_N} = \dot{V}_{N,CH_4} \cdot \frac{293,15}{293,15} = \dot{V}_{N,CH_4} \quad (38)$$

Now we have to take into account losses of heat during combustion: in fact, for a generic steam generator, efficiency would be given as:

$$\eta = 1 - P_I - P_D - P_C \quad (39)$$

where:

- P_I represents the loss due to unburnt reactants (here is zero, since we are assuming the stoichiometric combustion);
- P_D is the loss due to dispersion;
- P_C is the loss “at the chimney”, due to the fact that for general purpose, we are interested in not leaving any residual thermal power to exhausts by exploiting it entirely. In our case, however, we don’t consider this loss, since we are not interested in exploiting this amount of power, our purpose is only to furnish the requested energy to demanding fluids, the remaining power can be “wasted”.

Therefore, the only contribution taken into account will be the one linked to dispersion. They can be taken from UNI TS 11300-2:2008:

Tipo di isolamento del mantello del generatore	Età del generatore	$P'_{gn,env}$ [%]
Generatore nuovo ad alto rendimento, ben isolato	Nuova installazione	1,72-0,44 $\log\Phi_{cn}$
Generatore ben isolato e mantenuto	Fino a 5 anni ben isolato	3,45-0,88 $\log\Phi_{cn}$
Generatore obsoleto e mediamente isolato	Da 6 a 11 anni mediamente isolato	6,90-1,76 $\log\Phi_{cn}$
Generatore obsoleto e privo di isolamento	Da 6 a 11 anni privo di isolamento	8,36-2,20 $\log\Phi_{cn}$
Generatore non isolato	Superiore ai 12 anni	10,35-2,64 $\log\Phi_{cn}$

Table 19 - Losses due to dispersion through the combustion chamber [51]

Assuming a chamber with the best conditions and evaluating the respective losses that are function of fuel power (in turn evaluated thanks to fuel flowrate and lower heating value), we have assumed that, since to supply the requested heat at the requested temperature we have to supply the already assessed fuel flowrate, to supply this heat plus the amount of power wasted in losses we have to furnish a fuel flowrate that is given by the following formula:

$$\dot{V}_{N,CH_4} = \frac{\dot{V}_{N,CH_4,stoich}}{\eta} \quad (40)$$

$$\dot{V}_{CH_4} = \frac{\dot{V}_{CH_4,st}}{\eta} \quad (41)$$

Air volume flowrate is evaluated from theoretical air, in turn evaluated from reaction of combustion:

$$A_{th} = 2 \cdot \left(1 + \frac{79}{21}\right) = 9,5 \frac{Nm_{air}^3}{Nm_{fuel}^3} \quad (42)$$

$$\dot{V}_{N,air} = 9,5 \cdot \dot{V}_{N,CH_4} \quad (43)$$

$$\dot{V}_{air} = \dot{V}_{N,air} \cdot \frac{293,15}{293,15} = \dot{V}_{N,air} \quad (44)$$

We can finally calculate the volume of the combustion chamber, by assuming a residence time of 0,5 s within the reactor and an average flowrate as follows:

$$\dot{V}_{ave} = \frac{\dot{V}_{fuel} + \dot{V}_{air}}{2} \quad (45)$$

$$V_{comb.chamber} = \dot{V}_{ave} \cdot 0,5 \text{ s} \quad (46)$$

Now, for all the scenarios analysed, we have all the information to evaluate the contribution to Levelized Cost of Electricity (LCOE) linked to the heat exchanger network.

5.2.8 Evaluation of the LCOE

For each scenario, in order to evaluate the LCOE we have firstly to assess the annuity, i.e. the total cost divided into a number of instalments equal to the number of years of the plant but taking also into account the discharge rate of the money. Each annuity is composed of a contribution due to capital costs and one linked to the operational costs.

By assuming a plant lifetime of 25 years [42], it can be possible to evaluate the annuity linked to the purchasing costs (CAPEX) thanks to the following formula:

$$Annuity_{CAPEX} = Y \cdot \frac{i \cdot (i + 1)^n}{(i + 1)^n - 1} \quad (47)$$

where:

- Y represents the total capital cost (in our case, the sum of the TASCs of the components);
- i represents the discharge rate of the money (in our case, the WACC);
- n is the lifetime of the plant (set to 25 years).

For the contribution of the operational costs (OPEX), instead, it is sufficient to assume a value for the cost of natural gas for industrial users: as found in [43], it depends on the annual consumption of gas; furthermore, we assume a net cost, not taking into account fees. From there, it is possible to evaluate the annuity as follows:

$$Annuity_{OPEX} = C_{nat.gas} \cdot \dot{V}_{CH_4} \cdot CF \cdot 8760 \frac{h}{year} \cdot 3600 \frac{s}{h} \quad (48)$$

where:

- $C_{nat.gas}$ is the cost founded on web [\$/m³];
- \dot{V}_{CH_4} is the fuel flowrate from calculation [m³/s];
- CF is the Capacity Factor, i.e. the percentage of time in which the plant is functioning. Although we have already explained that plant is elaborated in order to work in continuous mode, we have assumed a CF=80% to take into account maintenance and difficulties with combustion chambers.

Total annuity, as already explained, is calculated as:

$$Annuity = Annuity_{CAPEX} + Annuity_{OPEX} \quad (49)$$

By assuming a net electric power of 1,298 MW from the work of Tesio [2], it is finally possible to assess the LCOE related to the carbonator side heat exchanger network:

$$LCOE = \frac{Annuity}{1,298 \text{ MW} \cdot 8760 \text{ h} \cdot CF} \quad (50)$$

We can now analyse results obtained.

5.3 Results and final comments

Results obtained with methodologies explained in previous chapter are reported below.

Step	LCOE Scenario 1a	LCOE Scenario 1b	LCOE Scenario 2
1	32,38	32,38	32,38
2	32,85	32,85	32,85
3	34,12	34,12	34,12
4	36,49	36,49	36,49
5	41,92	41,92	43,35
6	42,45	42,45	44,75
7	45,02	41,64	48,80
8	-	41,09	-
9	-	36,34	-
10	-	54,61	-

Table 20 - LCOEs during simplifications (LCOE are in \$/MWh)

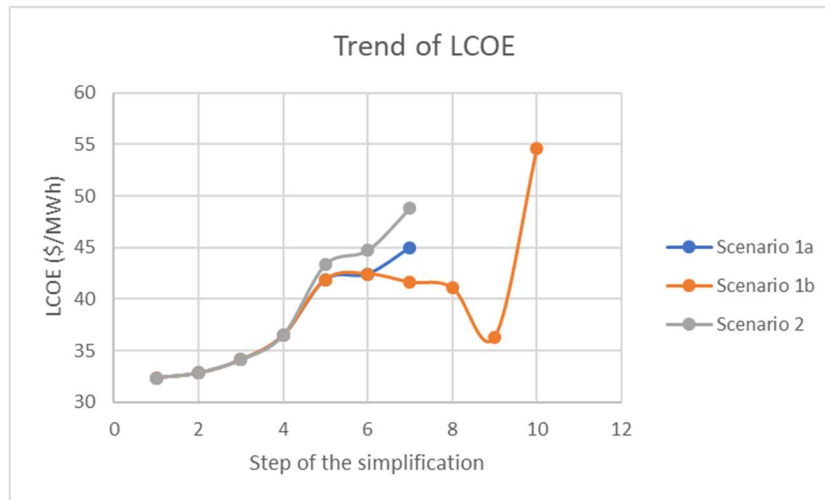
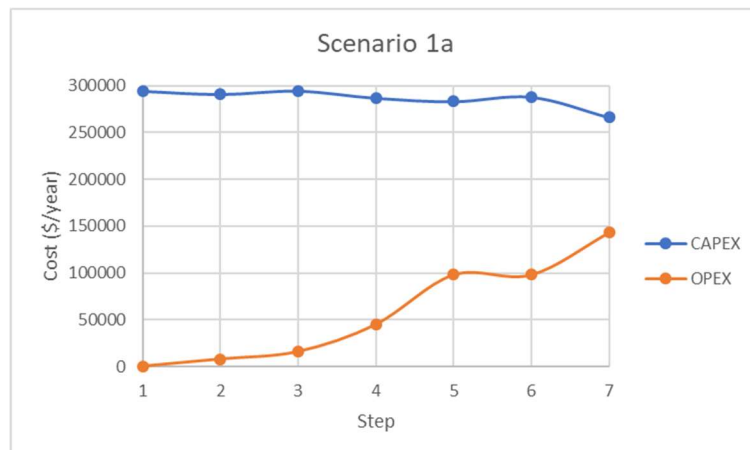


Figure 51 - Trend of LCOE during simplifications

As already said, it is not the total LCOE, but only the contribution linked to heat exchanger network, since it is the only thing that changes between different configurations. Before commenting the results, it's important to clarify two further aspects of the economic analysis carried out:

- near final steps of each Scenario, some designs haven't been analysed, since the re-addition of a heater would have further increased the cost, thus getting away from optimal point;
- at step 4 (the design after the 3rd simplification), it has been chosen the solution with the cooler as the best one; however, other solutions have been considered (increase of external requirements or addition of a heater), but none of them have been analysed economically since they appeared more expensive.

The first, most important comment to do is about the best design from an economic point of view: in fact, with assumptions made for the fuel and the type of exchangers, no one of the simplifications represent an improvement with respect to base equivalent case, which is our optimal configuration. This is due (for first simplifications) mainly to the CAPEX and OPEX trends, as we can observe from graphs below.



As we can observe for all the scenarios, in first simplifications, when CAPEX decrease, OPEX increase of a bigger amount, not allowing an improvement; moreover, moving forward OPEX increase more rapidly, while CAPEX decrease slowly or even increase: this is due to the fact that, making new removals, more external source needing means higher OPEX, whereas the re-addition of a heater/cooler influence CAPEX, sometimes not allowing a reduction. For Scenario 1b, last simplifications lead even to a situation in which OPEX become higher than CAPEX: this is linked to the fact that, as already said, for these last

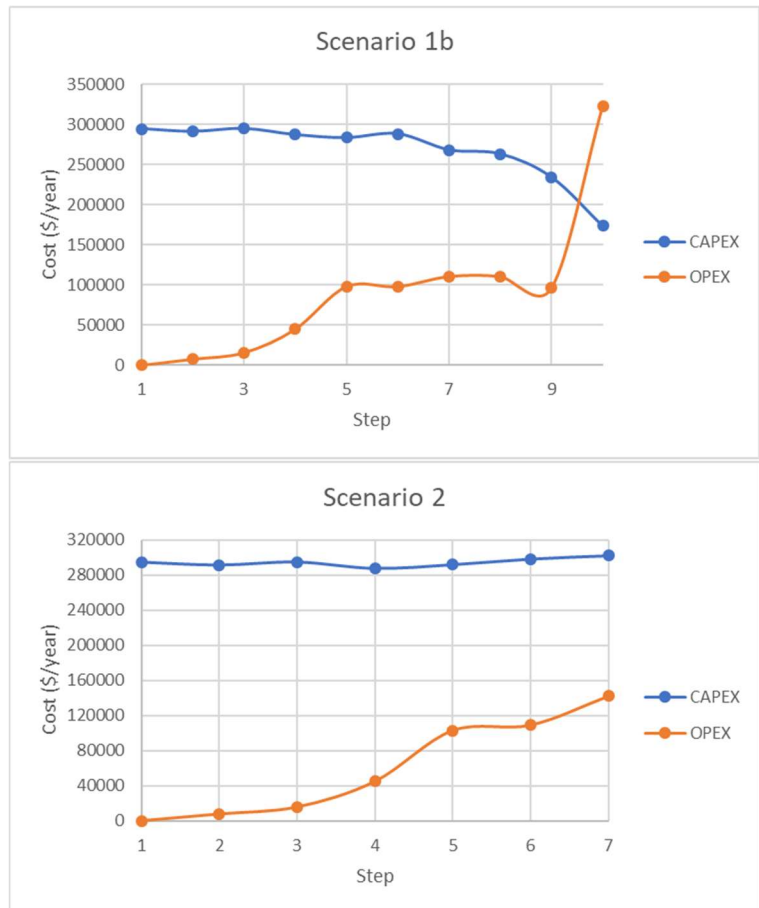


Figure 52-Trends of CAPEX and OPEX in different scenarios

removals we have tried to simplify the most expensive exchanger (and not the less powerful one), leading thus to a higher requirement increase.

Another intrinsic reason for which removals have not led to an improvement is the cost of natural gas: for chosen value of its price, in fact, even the first simplification (where a heat exchanger of 19,18 kW has been removed) doesn't allow to improve the situation, even if the worsening is quite low. In order to have an improvement in this first simplification (since for next ones, the increase of LCOE is too high to think about better economic conditions), we have to change type of natural gas considered or even the type of fuel. In the first case, since we have considered natural gas sold in Spain (since the pilot plant is planned to be installed in Seville), the only possibility is to consider natural gas from countries with lower prices (like Estonia, Romania and UK); we can observe different prices of gas for industrial users from table below.

Prezzi finali del gas naturale per i consumatori industriali nel 2017										
Prezzi al netto e al lordo delle imposte; c€/m ³										
	CONSUMATORI PER FASCIA DI CONSUMO ANNUO (migliaia di m ³)									
	< 26		26-263		263-2.627		2.627-26.268		26.268-105.072	
	NETTI	LORDI	NETTI	LORDI	NETTI	LORDI	NETTI	LORDI	NETTI	LORDI
Austria	45,37	63,01	35,95	51,36	28,12	42	23,02	35,23	21,38	32,85
Belgio	40,98	51,99	30,82	39,69	23,01	30,09	19,92	25,13	19,63	24,64
Bulgaria	29,21	36,43	27,34	34,19	23,8	29,88	19,13	23,53	18,26	21,93
Croazia	33,82	43,2	29,94	38,25	25,63	32,59	23,3	29,52	n.d.	n.d.
Danimarca	36,11	84,73	34,59	82,76	25,34	70,13	23,03	67,03	n.d.	n.d.
Estonia	30,25	40,96	27,75	38,34	25,23	35,2	24,22	33,99	24,21	33,59
Finlandia	n.d.	n.d.	39	70,35	34,92	65,26	n.d.	n.d.	n.d.	n.d.
Francia	44,44	60,12	36,03	49,79	29,88	41,67	23,47	30,02	21,02	24,62
Germania	41,36	54,28	32,68	43,96	28,71	39,25	23,03	32,49	19,87	28,71
Grecia	n.d.	n.d.	n.d.	n.d.	n.d.	n.d.	n.d.	n.d.	n.d.	n.d.
Irlanda	48,82	59,86	39,81	49,53	31,07	38,45	24,19	27,5	n.d.	n.d.
Italia	46,6	68,7	35,49	51,78	25,64	30,9	23,25	25,62	23,32	25,16
Lettonia	33,96	43,14	31,74	40,3	27,93	35,51	25,82	33,15	23,64	30,68
Lituania	32,3	46,16	29,69	42,15	27,69	39,07	25,33	35,54	n.d.	n.d.
Lussemburgo	38,49	42,67	36,8	40,42	33,24	36,29	23,31	25,19	n.d.	n.d.
Paesi Bassi	n.d.	n.d.	29,3	70,32	22,5	40,61	21,41	30,85	20,8	27,42
Polonia	36,6	45,75	34,12	42,79	28,37	35,72	23,61	29,49	20,02	25,01
Portogallo	51,83	72,93	38,03	49,64	28,23	35,73	24,25	30,44	23,93	29,5
Regno Unito	46,5	55,57	25,15	31,16	23,66	29,42	18,57	23,03	17,87	21,9
Cechia	35,87	44,95	27,67	35,03	24,26	30,9	22,97	29,34	23,66	30,18
Romania	22,9	38,64	20,55	35,66	18,22	32,97	16,92	28,3	16,47	25,52
Slovacchia	41,7	51,72	34,57	43,16	28,88	36,35	24,91	31,58	23,36	29,7
Slovenia	39,95	56,26	36,78	52,11	27,86	40,58	23,46	32,27	n.d.	n.d.
Spagna	39,7	48,73	37,16	45,66	29,34	36,18	26,13	32,31	22,56	27,99
Svezia	60,16	113,09	47,78	97,61	37,4	84,64	29,14	74,3	25,62	69,9
Ungheria	31,22	42,01	28,9	39,33	24,68	34,05	23,52	32,54	22,1	30,55
Unione eur	41,35	55,8	32,23	46,09	26,7	36,56	22,53	29,72	20,74	26,87
Area euro	42,12	57,66	33,92	49,37	27,49	37,66	23,22	30,33	21,25	27,11

(A) I dati relativi a Cipro e Malta non sono disponibili e quindi non sono presenti nella tavola.

Table 21 - Different prices of natural gas in EU countries [43]

Instead, if we decide to change fuel, we will lose the environmental advantage of the plant: in fact, we have decided to utilize natural gas since we are passing from a no-fuel, zero-emissions plant to a polluting one, so we have decided at least to consider the fuel with the lowest environmental impact; by changing it, our impact will increase and the plant contribute to the GHG reduction will be partially lost.

The best scenario is consequently the equivalent base case that, as already said, is a simplification of the reality, but the assumptions made (in particular concerning specific heats and the subdivision made for it) have allowed to have a situation very close to the real one: in other words, if we apply the design obtained for the equivalent case to the real situation (with real c_p), we'll obtain a

configuration in which the minimum temperature difference will be no longer maintained, but the “error” will be so small that it can be neglected.

As we can observe from figure above, in fact, the exchangers coincide with the equivalent case and temperature differences are almost equal to the ones from it, except for the heat exchanger connecting $C_6H_6,cond$ and C_6H_6,eva with a power of 234 kW above the 2nd pinch point: for this component, minimum temperature difference is not respected ($\Delta=223,8-216,4=7,4^\circ C < 15^\circ C$), so it becomes a question of deciding whether to choose a design with a higher number of exchangers but minimum difference respected or one with a violation of the pinch point difference but with simpler network. It has been also tried to modify the split of involved fluid (C_6H_6,eva) in order to establish again the minimum temperature difference of $15^\circ C$, but as a result, to solve the problem on that specific exchanger has only moved the problem toward exchangers along the remaining splits, even giving some infeasible results.

Since we haven't obtained any improvement in the simplification process, it can be interesting to investigate how the number of operation hours affects the simplification convenience: for all the calculations made above, in fact, we have assumed a capacity factor of 80% but applied on the entire number of hours in a year (8760), as if it was operating continuously (one of the hypothesis taken from Tesio's work was exactly about it). Now, in order to see a sort of improvement, we have assumed to reduce the number of hours; the results obtained are reported in the graph below.

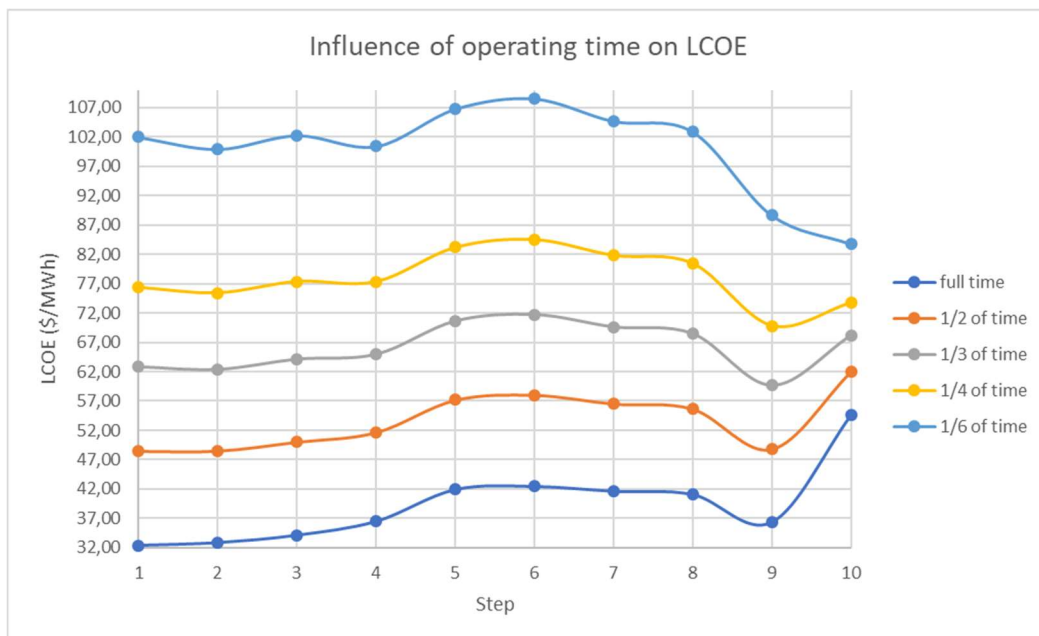


Figure 54 - LCOE as a function of operating time during simplification process

As we can observe, at full time (8760 hours), at half of the time (4380 hours) and at 1/3 of the time (2920 hours), the removal of the first exchanger hasn't produced any improvement in the LCOE; to see it, we have to consider only 1/4 of the full time (2190 hours), for which finally a short

improvement passing from base case to next design can be observed. The improvement trend can be further enhanced by considering 1/6 of the full time (1460 hours); if we had continued the reduction of time, we would have even obtained a situation in which the improvement would have moved to next removals. Another effect that can be noticed in the graph is that, by reducing the time, in some simplifications there is the formation of local minimum points; this is mainly linked to the fact that, while operational hours influence in a linear way the operational costs which, for example, in the 3rd simplification has not increased since we have added a cooler, CAPEX of the exchangers increase because of increased fluxes, but the addition of a cooler has a cost that is lower than the one of an internal exchanger (as the one removed), so also CAPEX have been reduced. This explanation is valid also for other local minima.

Of course, this methodology has the counter-effect of increasing the value of LCOE: in fact, to have the same configuration from the point of view of the temperatures, mass fluids flowrates have to be multiplied by a factor given by:

$$\text{factor of proportionality} = \frac{8760}{\text{hours of operation}} \quad (51)$$

For example, if we reduce the time to a half of full time, our factor of proportionality has to be 2, so mass flowrates will be twice the original value. As a consequence, also heat exchangers powers will be multiplied of the same factor, increasing thus the CAPEX. For the same reason, also net power produced by the plant will increase of the same factor, but the electricity produced (i.e. the value for which we have divided the total annuity to obtain the LCOE) will be the same, since the number of hours compares as a term in its calculation reduced of the same factor. OPEX will be almost independent on this change, since flowrate of flue gases will change because of the change of heaters power, but the fuel flowrates will be dependent also from hours of operation, so the variation is almost cancelled (not at all, since the dependency on the flue gases flowrate is not linear). For all these reasons, this solution is useful to see a sort of improvement in the removal, but it is useless for the improvement of the value of LCOE, since it is increased.

Conclusions

Finally, we can summarize what we have done in this work and describe the main steps of the analysis carried out.

First, we have explained the main features of SOCRATCES project, in particular concerning the CaL process and technology involved; then, after a brief presentation of the main possibilities of integration analysed in literature between CSP-CaL process and power cycles, this work has focused on the integration of Organic Rankine Cycles, about which a short explanation has been provided.

At this point, starting from optimal results obtained in previous works, a first attempt of heat exchanger network design has been made. However, since the resulting configuration showed a too high number of exchangers, the situation has been simplified by evaluating equivalent specific heat capacities for fluids in order to lower the number of couplings.

The resulting scenario has been then simplified with exchangers removals, in order to establish, thanks to suitable economic methodologies that permits to evaluate the contribution to LCOE from heat exchangers, which configuration is the best from the point of view of costs. It was found out that the best situation is the base one with equivalent heat capacities. This fact is mainly linked to the choice of external supply of heat, so an improvement in the simplification could be found by choosing another adequate type of fuel; therefore, this aspect could be interesting in a next work about these arguments.

In the end, it has been tried to apply the configuration obtained for equivalent base case (i.e. the best one) to the real case with real fluids, but we have obtained a violation of minimum temperature difference (since it has been obtained for a simplified, not realistic situation); also by trying to change split percentages of the fluids involved, the situation had not improved. Further studies can also start from this point, for example changing the type of organic fluid involved (here benzene has been considered, but in the thesis used as starting point there are many other ORC fluids analysed and for which optimal results are provided) and comparing the best designs obtained from an economic point of view, in order to establish which one is the simplest and whether there could be an improvement with removals or not. Also, a further analysis on the optimal time of functioning can be a good starting point for next works.

References

- [1] A. Gil, M. Medrano, I. Martorell, A. Lázaro, P. Dolado, B. Zalba e F. L. Cabeza, «State of the art on high temperature thermal energy storage for power generation. Part 1 - Concepts, materials and modellization,» *Renewable and Sustainable Energy Reviews*, vol. 14, n. 1, pp. 31-55, 2010.
- [2] U. Tesio, V. Verda e E. Guelpa, «Power generation alternatives for small scale concentrated solar power plants with energy storage based on Calcium-Looping,» 2018.
- [3] A. Alovio, R. Chacartegui e V. Verda, «Process Integration Of A Thermochemical Energy Storage System Based On Calcium Looping Incorporating Air/CO₂ Cycles In CSP Power Plants,» 2015.
- [4] G. Mohan, M. Venkataraman e J. Coventry, «Sensible energy storage options for concentrating solar power plants operating above 600 °C,» *Renewable and Sustainable Energy Reviews*, 2019.
- [5] A. Gil, M. Medrano, I. Martorell, X. Potau e F. L. Cabeza, «State of the art on high-temperature thermal energy storage for power generation. Part 2 - Case studies,» *Renewable and Sustainable Energy Reviews*, vol. 14, pp. 56-72, 2010.
- [6] B. Zalba, J. Marín, L. Cabeza e H. Mehling, «Review on thermal energy storage with phase change: materials, heat transfer analysis and applications,» *Applied Thermal Engineering*, vol. 23, n. 3, pp. 251-283, 2003.
- [7] K. Nithyanandam e R. Pitchumani, «Design of a latent thermal energy storage system with embedded heat pipes,» *Applied Energy*, vol. 126, pp. 266-280, 2014.
- [8] P. Pardo, A. Deydier, Z. Anxionnaz-Minvielle, S. Rougé, M. Cabassud e M. Cognet, «A review on high temperature thermochemical heat energy storage,» *Renewable and Sustainable Energy Reviews*, vol. 32, pp. 591-610, 2014.

- [9] C. Ortiz, R. Chacartegui, J. Valverde, A. Alovio e J. Becerra, «Power cycles integration in concentrated solar power plants with energy storage based on calcium looping,» *Energy Conversion and Management*, vol. 149, pp. 815-829, 2017.
- [10] C. Ortiz, J. Valverde, R. Chacartegui, L. Perez-Maqueda e P. Giménez, «The Calcium-Looping (CaCO₃/CaO) process for thermochemical energy storage in Concentrating Solar Power plants,» *Renewable and Sustainable Energy Reviews*, vol. 113, pp. 1-18, 2019.
- [11] T. Shimizu, T. Hiram, H. Hosoda, K. Kitano, M. Inagaki e K. Tejima, *Chemical Engineering Research and Design*, vol. 77, pp. 62-68, A Twin Fluid-Bed Reactor for Removal of CO₂ from Combustion Processes.
- [12] A. Alovio, R. Chacartegui, C. Ortiz, J. Valverde e V. Verda, «Optimizing the CSP-Calcium Looping integration for Thermochemical Energy Storage,» *Energy Conversion and Management*, vol. 136, pp. 85-98, 2017.
- [13] F.-C. Yu e L.-S. Fan, «Kinetic Study of High-Pressure Carbonation Reaction of Calcium-Based Sorbents in the Calcium Looping Process (CLP),» *Industrial & Engineering Chemistry Research*, vol. 50, pp. 11528-11536, 2011.
- [14] H. Canière, A. Willockx, E. Dick e M. De Paep, «Raising cycle efficiency by intercooling in air-cooled gas turbines,» *Applied Thermal Engineering*, vol. 26, n. 16, pp. 1780-1787, 2006.
- [15] R. Padilla, Y. Too, R. Benito e W. Stein, «Exergetic analysis of supercritical CO₂ Brayton cycles integrated with solar central receivers,» *Applied Energy*, vol. 148, pp. 348-365, 2015.
- [16] *SOCRATCES project presentation.*
- [17] W. Wentworth e E. Chen, «Simple thermal decomposition reactions for storage of solar thermal energy,» *Solar Energy*, vol. 18, n. 3, pp. 205-214, 1976.
- [18] S. Edwards e V. Materić, «Calcium looping in solar power generation plants,» *Solar Energy*, vol. 86, pp. 2494-2503, 2012.

- [19] R. Chacartegui, A. Alovio, C. Ortiz, J. Valverde, V. Verda e J. Becerra, «Thermochemical energy storage of concentrated solar power by integration of the calcium looping process and a CO₂ power cycle,» *Applied Energy*, vol. 173, pp. 589-605, 2016.
- [20] C. Ortiz, M. Romano, J. Valverde, M. Binotti e R. Chacartegui, «Process integration of Calcium-Looping thermochemical energy storage system in concentrating solar power plants,» *Energy*, vol. 155, pp. 535-551, 2018.
- [21] T. Hung, T. Shai e S. Wang, «A review of organic Rankine cycles (ORCs) for the recovery of low-grade waste heat,» *Energy*, vol. 22, n. 7, pp. 661-667, 1997.
- [22] J. Facão e A. Oliveira, «Analysis of energetic, design and operational criteria when choosing an adequate working fluid for small ORC systems,» in *ASME 2009 International Mechanical Engineering Congress & Exposition (IMECE2009)*, Lake Buena Vista, Florida, USA, 2009.
- [23] E. Macchi, «Theoretical basis of the Organic Rankine Cycle,» in *Organic Rankine Cycle (ORC) Power Systems - Technologies and Applications*, Kent Woodhead Publishing, 2017, pp. 3-24.
- [24] B. Tchanche, G. Papadakis, G. Lambrinos e A. Frangoudakis, «Fluid selection for a low-temperature solar organic Rankine cycle,» *Applied Thermal Engineering*, vol. 29, pp. 2468-2476, 2009.
- [25] S. Quoilin, M. Van Den Broek, S. Declaye, P. Dewallef e V. Lemort, «Techno-economic survey of Organic Rankine Cycle (ORC) systems,» *Renewable and Sustainable Energy Reviews*, vol. 22, pp. 168-186, 2013.
- [26] Y. Lara, P. Lisbona, A. Martínez e M. Romeo, «Design and analysis of heat exchanger networks for integrated Ca-looping systems,» *Applied Energy*, vol. 111, pp. 690-700, 2013.
- [27] V. Verda e E. Guelpa, *Metodi Termodinamici per l'uso efficiente delle Risorse Energetiche*, Società Editrice Esculapio, 2013.
- [28] J. Wimer e W. Summers, «Quality Guideline for Energy System Studies: Cost Estimation Methodology for NETL Assessments of Power Plant Performance,» DOE/NETL, 2011.

- [29] D. Bhattacharyya, J. Shaeiwitz, W. Whiting, R. Bailie e R. Turton, «Appendix A. Cost Equations and Curves for the CAPCOST Program,» in *Analysis, Synthesis, and Design of Chemical Processes (Fourth Edition)*, Prentice Hall, 2012, pp. 909-940.
- [30] M. Lazova, H. Huisseune, A. Kaya, S. Lecompte, G. Kosmadakis e M. De Paepe, «Performance Evaluation of a Helical Coil Heat Exchanger Working under Supercritical Conditions in a Solar Organic Rankine Cycle Installation,» *energies*, 2016.
- [31] F. Arrieta e L. Moreira, «Optimization, thermodynamic and economic analysis of a regenerative ORC for WHR in manufacturing process of cement,» in *THE 31ST INTERNATIONAL CONFERENCE ON EFFICIENCY, COST, OPTIMIZATION, SIMULATION AND ENVIRONMENTAL IMPACT OF ENERGY SYSTEMS*, GUIMARÃES, PORTUGAL, 2018.
- [32] M. Marchionni, G. Bianchi, M. Konstantinos e A. Savvas, «Techno-economic comparison of different cycle architectures for high temperature waste heat to power conversion systems using CO₂ in supercritical phase,» *Energy Procedia*, vol. 123, pp. 305-312, 2017.
- [33] H. P. Corporation, *The Basics of AIR-COOLED HEAT EXCHANGERS*.
- [34] «The Engineering ToolBox,» [Online]. Available: https://www.engineeringtoolbox.com/metal-corrosion-resistance-d_491.html.
- [35] K. Albrecht e C. Ho, «Design and operating considerations for a shell-and-plate, moving packed-bed, particle-to-sCO₂ heat exchanger,» *Solar Energy*, vol. 178, pp. 331-340, 2019.
- [36] «Chemical Engineering,» [Online]. Available: <https://www.chemengonline.com/2019-cepci-updates-january-prelim-and-december-2018-final/>.
- [37] «Il Sole 24 Ore,» [Online]. Available: <https://mercati.ilsole24ore.com/obbligazioni/spread/GBITL10J.MTS>. [Consultato il giorno 25 Ottobre 2019].
- [38] KPMG, «KPMG,» [Online]. Available: <https://assets.kpmg/content/dam/kpmg/nl/pdf/2018/advisory/equity-market-risk-premium-july-2018.pdf>.

- [39] «Il Sole 24 Ore,» [Online]. Available: <https://mercati.ilsole24ore.com/tassi-e-valute/tassi/irs>. [Consultato il giorno 25 Ottobre 2019].
- [40] «The Engineering Toolbox,» [Online]. Available: https://www.engineeringtoolbox.com/adiabatic-flame-temperature-d_996.html.
- [41] «Increase Performance,» [Online]. Available: <http://www.increase-performance.com/calc-flue-gas-prop.html>.
- [42] «SolarPACES - Solar Power & Chemical Energy Systems,» [Online]. Available: <https://www.solarpaces.org/what-are-the-pros-and-cons-of-longer-solar-contracts/>.
- [43] «ARERA - Autorità di Regolazione per Energia Reti e Ambiente,» [Online]. Available: <https://www.arera.it/it/dati/gpcfr2.htm>.
- [44] A. Abedin, «A Critical Review of Thermochemical Energy Storage Systems,» *The Open Renewable Energy Journal*, vol. 4, n. 1, pp. 42-46, 2011.
- [45] J. Blamey, E. Anthony, J. Wang e P. Fennell, «The calcium looping cycle for large-scale CO₂ capture,» *Progress in Energy and Combustion Science*, vol. 36, pp. 260-279, 2010.
- [46] M. Benitez-Guerrero, J. Valverde, P. Sanchez-Jimenez, A. Perejon e L. Perez-Maqueda, «Multicycle activity of natural CaCO₃ minerals for thermochemical energy storage in Concentrated Solar Power plants,» *Solar Energy*, vol. 153, pp. 188-199, 2017.
- [47] J. Sever, «Calix Calciner: A Green Application in the Production of Magnesium,» in *Drying, Roasting, and Calcining of Minerals*, Wiley, 2015, pp. 121-126.
- [48] A. Shimizu, T. Yokomine e T. Nagafuchi, «Development of gas–solid direct contact heat exchanger by use of axial flow cyclone,» *International Journal of Heat and Mass Transfer*, vol. 47, pp. 4601-4614, 2004.
- [49] «Commercial Heat Exchanger - Efficient Bulk Solids Heating | Solex - Solex,» Solex, [Online]. Available: <https://www.solexthermal.com/products-solutions/heating/>. [Consultato il giorno 22 09 2019].

[50] M. Astolfi, «Technical options for Organic Rankine Cycle systems,» in *Organic Rankine Cycle (ORC) Power Systems - Technologies and Applications*, Kent Woodhead Publishing, 2017, pp. 67-89.

[51] «My Green Buildings,» [Online]. Available:
<http://www.mygreenbuildings.org/2013/05/25/perdite-al-mantello-caldaia.html>.

Ringraziamenti

Sono tante le persone che dovrei ringraziare in questi anni per avermi aiutato a superare i momenti difficili che questa università (e non solo) mi ha dato. Anche se sarebbe servito molto più spazio di quello fornito da questa Tesi per ringraziarle tutte a dovere, vorrei che una parte di questo mio piccolo traguardo fosse condivisa con coloro che mi sono stati vicini nei momenti bui, quando pensavo di fermare tutto, ma anche nei momenti di gioia, quando una battuta scambiata, un piccolo successo o il togliersi delle soddisfazioni mi hanno infuso maggior forza nel proseguire questo cammino.

Ai miei compagni di università, con cui ho condiviso gioie ma soprattutto fatiche, e grazie ai quali l'avermi tirato su con una battuta o l'avermi fatto sentire come un amico ha fatto sì che io non impazzissi del tutto dentro quelle quattro mura e non crollassi dopo i miei fallimenti scolastici. Grazie in particolare a tutti coloro che c'erano fin dall'inizio, i New Balancers, per aver reso indimenticabili questi anni. A Umberto, per avermi mostrato la luce di questa Tesi quando ad un certo punto vedevo solo nebbia e per essere sempre stato disponibile e paziente nei confronti dei miei momenti di sclero.

Ai miei compagni di calcio, per essere stati più di una semplice squadra di pazzi criminali male assortita, ma una seconda famiglia, che mi ha aiutato a risollevarmi quando nella mia vita tutto sembrava crollare. Grazie soprattutto a quelli del gruppo "storico", del nocciolo duro compagno di tante (forse troppe) birre; a Pato e a Cava, per essere stati più di due mentori e per avermi supportato in quel salto di carattere che mi era necessario per farcela dopo tutto quanto passato, a Tonio, Vigo, Luca, Moresco, Vins, Fava, Pupo e Dani, per le mille risate che mi avete fatto fare in tutti questi anni.

Agli amici del Liceo, perché dopo tutti questi anni ancora mi sopportano e ancora mi fanno ridere quando ci vediamo, come se non fosse mai passato il tempo. A Ste e a Edo, gli Zì, per avermi sempre strappato una risata quando ne avevo bisogno; a Valentina, per essere stata in tutti questi anni non solo la persona capace di trainarmi oltre la confusione dentro il mio cervello ed aiutarmi a passare questi anni scolastici, ma anche capace di ascoltarmi quando avevo solo bisogno di uno sfogo; a Giulia, per essere stata una roccia quando io forse ero a pezzi ed essere stata un'amica migliore di quanto avrei mai potuto chiedere.

Agli amici di sempre, che in questi anni mi sono sempre stati vicini, hanno sempre sopportato il mio carattere chiuso e mi hanno aiutato a rialzarmi quando cadevo e crollavo. Agli amici di Leva, con i quali il tempo ci ha allontanato ma senza perderci mai, tornando sempre per fare serate epiche e risate che scaldano il cuore. Ad Andre, Giu, Mariano, Eleonora, Marco, Gian e Marti, per le mille avventure e risate vissute assieme (e per le altre mille che verranno); a Elena che, nonostante sia lontana nello spazio, mi è sempre rimasta vicina e c'è sempre stata nel momento del bisogno e dello sfogo. A Michi, Paola, Luca e a tutto il gruppo dei camminatori, perché è anche grazie a quell'esperienza estiva e alle gioie e all'affetto che mi avete infuso se ce l'ho fatta a superare il momento difficile arrivato subito dopo. A Chri, per essere sempre folle come lo sono io, per esserci sempre ed essere pronto a vivere mille avventure, non importa dove e non importa quando.

A tutta la famiglia: da quella fatta di cugini "conosciuti" da poco, ma che sembrano ormai farne parte da sempre con la loro vicinanza e il loro affetto, a quella allargata, per rendere ogni festività e ogni incontro una grande gioia e un'occasione per ridere insieme; un grazie in particolare ad Ondina e Monica, perché se io e Fede abbiamo avuto la peggiore delle perdite che la vita può darti ma non ci è mai mancato l'affetto di una "seconda mamma" e "seconda sorella", questo è grazie a voi. A Francesca, Giorgio e Antonietta, per non aver mai fatto mancare il vostro affetto in questo anno difficile ed esserci sempre stati; e a Fabio, per essermi sempre stato vicino anche solo con l'affetto di qualche parola giusta al momento giusto, e a mia madrina Manu, perché nessuno forse lo sa, ma se ho sconfitto la mia fobia della guida è solo grazie a te e all'incoraggiamento che mi hai dato.

A mio padre, nei confronti del quale spesso i nostri caratteri entrambi chiusi e divergenze nel corso degli anni hanno portato a litigare, ma a cui voglio bene e senza l'affetto del quale non ce l'avrei fatta a superare l'anno scorso.

A mia sorella, compagna di mille litigi e di carattere diametralmente opposto al mio, ma che nel momento più buio, nonostante tutto il dolore che pure lei provava, ha saputo rialzarsi, rialzarmi e reggermi mentre la corrente cercava di spazzarmi via. Non sono mai stato bravo a comunicarti il mio affetto, ma sappi che non potrò mai dimenticare tutto ciò che hai fatto in quest'ultimo anno per noi.

E infine, l'unico grazie che non avrei voluto mai fare così, il motivo per cui fino all'ultimo ho rimandato questo momento. Mi trovo qua davanti allo schermo, pensando a cosa dirti, cosa comunicarti che già non sai: sai già che quel giorno mancherai un sacco, che mentre guarderò il pubblico prima di iniziare a parlare vedrò inevitabilmente quel posto vuoto vicino a Fede e a papà,

e che quello forse sarà il momento più terribile di tutti, perché in qualche modo non ti vedrò tentare di non commuoverti perché ti avrei sgridato (ma alla fine guardandoti mi sarei commosso anch'io); sai già che se in quei due/tre momenti in cui pensavo di mollare non l'ho fatto, è grazie soprattutto a te, all'amore di mamma che non mi hai mai fatto mancare, e che quindi se mi trovo qua a raggiungere questo obiettivo lo devo tutto a te. Forse un giorno riuscirò a mostrarti questo traguardo, e potrò finalmente vedere la tua gioia che mi avrebbe ripagato di tutte le fatiche; anzi, sono sicuro che quel giorno arriverà. Fino ad allora, grazie di tutto. Ciao Giusy. Ciao mamma.